Large-Sample Performance of Blind and Group-Blind Multiuser Detectors: A Perturbation Perspective

Zhengyuan Xu, *Senior Member, IEEE,* and Xiaodong Wang, *Member, IEEE*

***Abstract*—In blind and group-blind multiuser detection, different detectors can be designed using either the sample data covariance matrix directly or its eigencomponents. Due to finite-sample effect in practice, their performance deviates from the corresponding optimum. A perturbation technique is developed rigorously and systematically to analyze those detectors in this work. Subject to the assumption that the first-order perturbation dominates, corresponding results can be applied to a practical system of a given sample size. In particular, performance of the following typical detectors is studied for either flat or estimated multipath channels: direct-matrix-inversion (DMI) blind minimum mean-square error (MMSE) detector, subspace blind MMSE detector, direct zero-forcing (ZF) detector, subspace ZF detector, and group-blind hybrid detector. Simulation examples further verify various analytical results.**

***Index Terms*—Asymptotic performance, multiuser detection, perturbation analysis, subspace decomposition.**

I. Introduction

In recent two decades, design of blind multiuser detectors to detect code-division multiple-access (CDMA) signals has received considerable attention [1]–[5]. Its main focus is to design satisfactory detectors without relying on any training sequence. Blind linear detectors are very attractive because of their low complexity and ease of implementation [6]. Of particular interest are minimum mean-square error (MMSE) and zero-forcing (ZF) detectors.

There exist different strategies in designing detection techniques for different communication scenarios. If a transmitted signal experiences only flat fading, the direct MMSE detection can be performed based on the inverse of the received data covariance matrix and the code waveform of the desired user [1], [6]. This scheme is termed as direct-matrix-inversion (DMI) detection. It requires spreading codes of the desired user. Applying eigenvalue decomposition (EVD) on the data covariance matrix and invoking orthogonality between the signal subspace and noise subspace, an equivalent subspace MMSE detection method follows [2], [7]. Similarly, spreading codes of the desired user are necessary for reconstruction of the desired symbol's waveform. If the system noise is negligible, a ZF detector can provide better performance. It utilizes code waveforms of all users. In the case when only spreading codes of some users are known, then a group-blind MMSE detector can be built by constraining the response from other users in the group to be zero while adopting the MMSE criterion [8]. It uses spreading codes of all known users. A group-blind ZF detector can also be constructed and has been shown to have the same form and code requirement as a blind ZF detector. In a multipath fading environment, the signature waveform of the desired signal becomes a convolution of the spreading codes and channel coefficients and is no longer known *a priori*. Therefore, to design different detectors, channel parameters are usually estimated first to reconstruct the signature waveform. The subspace technique is capable of fulfilling this task [7], [9]. Then following similar procedures as above, those linear detectors can be constructed based on reconstructed signal waveforms.

It can be observed that in designing the afore-mentioned detectors either with or without multipath fading, the data covariance is directly or indirectly involved. Although performance of different detectors can be assessed under perfect conditions, in practice it is commonly affected by various factors. The size of collected data samples N causes direct perturbation to data covariance and thus degrades detectors' performance. To gain some insight into its sensitivity to the sample size, a number of papers have appeared to analyze the asymptotic performance of different detectors with random long spreading sequences when the number of users J grows without bound and the ratio of J to the processing gain M is fixed [10]–[14].

Different from those approaches, our current work focuses on asymptotic performance of blind and group-blind multiuser detectors when short spreading codes are used and when the detectors are estimated from received signals. Although their performance in terms of the output signal to interference plus noise ratio (SINR) and the bit-error rate (BER) has been analyzed from the central limit theorem in [15], those results are only applicable for flat-channel cases assuming perfect channel knowledge.

We perform various systematic analyses for both flat-channel and multipath-channel scenarios from a perturbation perspective. In the presence of multipath distortion, channel parameters are estimated and resulting errors affect different detectors. Thus, joint analysis of detectors and channel estimators appears necessary. In practice, channel estimation error stems from insufficient number of data samples. The received signal covariance estimated from large data samples is only slightly perturbed if compared with its ideal counterpart, leading to application of a perturbation technique. In fact, the requirement for

Manuscript received January 20, 2003, revised April 16, 2004. The work of Z. Xu was supported by the U.S. National Science Foundation under Grant NSF-CCR 0207931. The work of X. Wang was supported by the U.S. National Science Foundation under Grants CCR–0225721 and CCR-0225826.

Z. Xu is with the Department of Electrical Engineering, University of California, Riverside, CA 92521 USA (e-mail: dxu@ee.ucr.edu).

X. Wang is with the Department of Electrical Engineering, Columbia University, New York, NY 10027 USA (e-mail: wangx@ee.columbia.edu).

Communicated by V. V. Veeravalli, Associate Editor for Detection and Estimation.

Digital Object Identifier 10.1109/TIT.2004.834853

a large sample size can be relaxed. Estimated covariance based on only a few hundred samples is a fairly good approximation for the ideal one according to the detectors' performance. Under a Gaussian assumption in [15], up to the second-order statistics of each perturbed detector suffice to describe each practical detector. Although in our approach we do not elaborate on detectors' asymptotic distributions, we evaluate up to the second-order statistics required for evaluation of SINRs. Therefore, despite different viewpoints, it is not surprising that our results for systems without multipath distortion are observed to be consistent with those in [15] according to simulation. However, it is worth to point out that we provide a systematic analytical method suitable for not only flat-channel cases, but also multipath scenarios where channel parameters are estimated with unavoidable errors. In addition to estimation errors in data covariance, those errors affect detection performance as well. Hence, joint performance study is conducted in the current work.

In general, perturbations may arise from various sources such as system noise, modeling error, or finite samples processed. Perturbation technique has been successfully applied in many applications to analyze the effects of some of these factors, such as in direction-of-arrival (DOA) estimation to obtain the estimation error [16], in subspace channel estimation to derive statistics of the channel estimator [17], [18]. Here, we particularly examine asymptotic properties (large sample size N) of the following blind linear detectors for either flat or multipath channels: DMI MMSE detector, subspace MMSE detector, subspace ZF detector, and group-blind hybrid detector which are proposed in [7] and [8], respectively. SINR and BER are still adopted as two measures for both qualitative and quantitative performance [15]. For large N, the data covariance matrix gets perturbed. Thus, its eigencomponents are perturbed as well, whose correspondence to the perturbation of the data covariance is explicitly exposed according to perturbation theory. After applying the statistics of sample-based estimated covariance [19] and deriving a vector-form variant, SINRs are derived as functions of the sample size and other system parameters. Compared with associative ideal detectors, those data-based detectors show performance degradation due to sample effect. It is found that resulting errors in signal power and interference plus noise power are inversely proportional to the sample size. Therefore, as sample size increases, those errors tend to be negligible, making the performance of each detector converge to that of the ideal counterpart. When multipath propagation occurs, perturbation in each of the data-based detectors stems from the channel estimation error as well. In such a scenario, we analyze the detection performance if channel parameters are estimated by a typical subspace technique [20].

The organization of this paper is as follows. Section II first presents a CDMA system model and provides a brief review of the afore-mentioned blind linear detectors. Detailed analyses of the effect of the sample size are performed in Section III for both flat and multipath channels. Simulation examples are provided in Section IV. Finally, some concluding remarks are made in Section V.

II. System Model and Different Linear Detectors

Consider a synchronous CDMA system with J users. All discussions can be easily extended to an asynchronous system based on the delay for each user. User j $(j=1,\dots,J)$ is assigned spreading codes $c_j(k)$ $(k=1,\dots,M)$ of length M to spread its information symbol $b_j(n)$. Let the chip sequence be transmitted through a multipath channel with a baseband chip rate discrete-time impulse response $g_j(n)$. Then the received discrete-time signal at the chip-rate receiver is [3]

$$y(n)=\sum_{j=1}^{J}\sum_{l=-\infty}^{\infty}\sum_{m=-\infty}^{\infty}b_j(l)g_j(m)c_j(n-m-lM)+v(n) \tag{1}$$

where $b_j(n)$ is assumed to have zero-mean and variance $\sigma_{b_j}^2$, $v(n)$ is zero-mean additive white Gaussian noise (AWGN) with variance σ_v^2.

The discrete-time model can be easily formulated into a matrix/vector representation. Assume all channels $g_j(n)$ have maximum order $q \ll M$. After collecting M measurements in a vector $\boldsymbol{y}_n$ and neglecting intersymbol interference (ISI), then convolution in (1) can be written as matrix/vector multiplication [3]

$$\boldsymbol{y}(n)=\sum_{j=1}^{J}\boldsymbol{h}_j b_j(n)+\boldsymbol{v}(n), \boldsymbol{h}_j=\boldsymbol{C}_j\boldsymbol{g}_j \tag{2}$$

where

$$\boldsymbol{C}_j=\begin{bmatrix} c_1(1) & & \mathbf{0} \\ \vdots & \ddots & \\ \vdots & & c_1(1) \\ \vdots & & \vdots \\ c_1(M) & \cdots & c_1(M-q)\end{bmatrix}, \quad \boldsymbol{g}_j=\begin{bmatrix} g_j(0)\\ \vdots \\ g_j(q)\end{bmatrix}. \tag{3}$$

Extension of the data model (2) to an asynchronous system with an arbitrary channel order is much straightforward by considering ISI for each user. As a special case, the model (2) can also describe the system without multipath fading by setting $\boldsymbol{g}_j$ to be a scalar and correspondingly $\boldsymbol{C}_j$ to a vector.

According to (2), different detectors can be designed to detect $b_j(n)$. Without loss of generality, assume user 1 is the desired user, and $\sigma_{b_1}^2 = 1$. The linear MMSE detector for user 1 is defined as

$$\boldsymbol{m}_1=\min_{\boldsymbol{m}} E\left\{\left|b_1(n)-\boldsymbol{m}^H\boldsymbol{y}_n\right|^2\right\}=\boldsymbol{R}^{-1}\boldsymbol{h}_1 \tag{4}$$

where $\boldsymbol{R}=E\left\{\boldsymbol{y}_n\boldsymbol{y}_n^H\right\}$, superscript ^{H} represents complex conjugate transpose. This detector requires direct inversion of matrix $\boldsymbol{R}$ and is called a DMI MMSE detector.

The MMSE detector $\boldsymbol{m}_1$ can also be expressed in terms of the signal subspace components of $\boldsymbol{R}$. Let the EVD of $\boldsymbol{R}$ be

$$\begin{aligned}\boldsymbol{R}&=\boldsymbol{U}_s\boldsymbol{\Lambda}_s\boldsymbol{U}_s^H+\boldsymbol{U}_n\boldsymbol{\Lambda}_n\boldsymbol{U}_n^H\\ \boldsymbol{\Lambda}_s&=\operatorname{diag}\left\{\lambda_1^2,\dots,\lambda_J^2\right\}, \qquad \boldsymbol{\Lambda}_n=\sigma_v^2\boldsymbol{I}\end{aligned} \tag{5}$$

where $\boldsymbol{U}_s$ and $\boldsymbol{U}_n$ represent the signal and noise subspaces, respectively. Invoking the orthogonality between $\boldsymbol{U}_n$ and $\boldsymbol{h}_1$, $\boldsymbol{m}_1$ is equivalent to the following form [7]:

$$\boldsymbol{m}_2 = \boldsymbol{U}_s \Lambda_s^{-1} \boldsymbol{U}_s^H \boldsymbol{C}_1 \boldsymbol{g}_1. \tag{6}$$

For distinction in description, we have used $\boldsymbol{m}_2$ to denote this subspace MMSE detector although it is theoretically the same as $\boldsymbol{m}_1$.

The ZF detector aims to eliminate multiple-access interference (MAI) together with ISI if it is present. For convenience, let us define

$$\boldsymbol{H} = [\boldsymbol{h}_1, \ldots, \boldsymbol{h}_J], \quad \boldsymbol{b}_n = [b_1(n), \ldots, b_J(n)]^T.$$

Then (2) can be written as

$$\boldsymbol{y}(n) = \boldsymbol{H}\boldsymbol{b}_n + \boldsymbol{v}_n. \tag{7}$$

Therefore, a ZF detector $\boldsymbol{d}_1$ satisfies $\boldsymbol{d}_1^H \boldsymbol{H} = \boldsymbol{e}_{J,1}$ where $\boldsymbol{e}_{J,1}$ is a unitary vector of length J with the first element to be 1. It is shown in [7] that it takes either a direct form

$$\boldsymbol{d}_1 = \boldsymbol{H}(\boldsymbol{H}^H \boldsymbol{H})^{-1} \boldsymbol{e}_{J,1} \tag{8}$$

or a subspace form

$$\boldsymbol{d}_2 = \boldsymbol{U}_s \boldsymbol{\Omega}^{-1} \boldsymbol{U}_s^H \boldsymbol{C}_1 \boldsymbol{g}_1, \ \ \boldsymbol{\Omega} = \boldsymbol{\Lambda}_s - \sigma_v^2 \boldsymbol{I} = \boldsymbol{\Lambda}_s - \frac{1}{L}\mathrm{tr}(\boldsymbol{\Lambda}_n)\boldsymbol{I} \tag{9}$$

where "tr" represents trace of a matrix, $L = M - J$.

In a case where only codes and channels from user 1 to user K $(K \leq J)$ are known, interference caused by those $K-1$ interfering users can be zero-forced while interference from remaining $J-K$ unknown users are suppressed by the group-blind linear hybrid detector according to the MMSE criterion. If signature waveforms of K users are collected in $\boldsymbol{H}_K = [\boldsymbol{h}_1, \ldots, \boldsymbol{h}_K]$, then such a detector is given by the following constrained MMSE criterion [8]:

$$\boldsymbol{w} = \arg \min_{\boldsymbol{w} \in range(\boldsymbol{H}_K)} E\left\{|b_1(n) - \boldsymbol{w}^H \boldsymbol{y}_n|^2\right\}, \quad \text{subject to } \boldsymbol{w}^H \boldsymbol{H}_K = \boldsymbol{e}_{K,1}^T. \tag{10}$$

The solution takes the following form based on the subspace decomposition of $\boldsymbol{R}$:

$$\boldsymbol{w} = \boldsymbol{U}_s \Lambda_s^{-1} \boldsymbol{U}_s^H \boldsymbol{H}_K \left[\boldsymbol{H}_K^H \boldsymbol{U}_s \Lambda_s^{-1} \boldsymbol{U}_s^H \boldsymbol{H}_K\right]^{-1} \boldsymbol{e}_{K,1}. \tag{11}$$

The term "hybrid" is due to adoption of both ZF and MMSE criteria at the same time. Accordingly, the detector is called a hybrid detector.

Those analytical expressions are derived based on ideal quantities. However, in practice, the data covariance matrix is estimated from N data vectors

$$\widehat{\boldsymbol{R}} = \frac{1}{N}\sum_{n=1}^{N} \boldsymbol{y}_n \boldsymbol{y}_n^H = \widehat{\boldsymbol{U}}_s \widehat{\boldsymbol{\Lambda}}_s \widehat{\boldsymbol{U}}_s^H + \widehat{\boldsymbol{U}}_n \widehat{\boldsymbol{\Lambda}}_n \widehat{\boldsymbol{U}}_n^H \tag{12}$$

with eigencomponents deviated from their theoretical values, where $\widehat{\boldsymbol{\Lambda}}_s$ and $\widehat{\boldsymbol{\Lambda}}_n$ contain J largest eigenvalues and L remaining eigenvalues of $\widehat{\boldsymbol{R}}$, respectively, $\widehat{\boldsymbol{U}}_s$ and $\widehat{\boldsymbol{U}}_n$ contain corresponding eigenvectors. Meanwhile, the subspace channel estimation method also employs the covariance matrix. Correspondingly, all previously discussed detectors are perturbed when compared with their ideal forms. Those equivalent MMSE detectors $\boldsymbol{m}_1$ and $\boldsymbol{m}_2$, or ZF detectors $\boldsymbol{d}_1$ and $\boldsymbol{d}_2$, may show different performance in the presence of covariance estimation error $\delta\boldsymbol{R} = \widehat{\boldsymbol{R}} - \boldsymbol{R}$ where a δ precedes $\boldsymbol{R}$ to represent perturbation. The same convention will follow in our later discussion.

For previously mentioned reasons, we assume N is sufficiently large, lending the perturbation technique directly applicable to our analysis. Instead of analyzing asymptotic distributions of detectors [15], we will derive the perturbation of each of them from a perturbation perspective. It will be shown that the eigencomponents of $\widehat{\boldsymbol{R}}$ which are perturbed play important roles.

With given N data vectors, the MMSE detectors $\boldsymbol{m}_1$ and $\boldsymbol{m}_2$ are implemented as

$$\widehat{\boldsymbol{m}}_1 = \widehat{\boldsymbol{R}}^{-1} \boldsymbol{C}_1 \widehat{\boldsymbol{g}}_1 \tag{13}$$

$$\widehat{\boldsymbol{m}}_2 = \widehat{\boldsymbol{U}}_s \widehat{\boldsymbol{\Lambda}}_s^{-1} \widehat{\boldsymbol{U}}_s^H \boldsymbol{C}_1 \widehat{\boldsymbol{g}}_1 \tag{14}$$

where $\widehat{\boldsymbol{g}}_1$ is an estimated channel vector. In two forms of the ZF detector, $\boldsymbol{d}_1$ explicitly requires $\boldsymbol{H}$. Therefore, the ZF detector is implemented in a direct form as

$$\widehat{\boldsymbol{d}}_1 = \widehat{\boldsymbol{H}}(\widehat{\boldsymbol{H}}^H \widehat{\boldsymbol{H}})^{-1} \boldsymbol{e}_{J,1} \tag{15}$$

or in a subspace form as

$$\widehat{\boldsymbol{d}}_2 = \widehat{\boldsymbol{U}}_s \widehat{\boldsymbol{\Omega}}^{-1} \widehat{\boldsymbol{U}}_s^H \boldsymbol{C}_1 \widehat{\boldsymbol{g}}_1. \tag{16}$$

The hybrid detector has a form

$$\widehat{\boldsymbol{w}} = \widehat{\boldsymbol{U}}_s \widehat{\boldsymbol{\Lambda}}_s^{-1} \widehat{\boldsymbol{U}}_s^H \widehat{\boldsymbol{H}_K} \left[\widehat{\boldsymbol{H}_K}^H \widehat{\boldsymbol{U}}_s \widehat{\boldsymbol{\Lambda}}_s^{-1} \widehat{\boldsymbol{U}}_s^H \widehat{\boldsymbol{H}_K}\right]^{-1} \boldsymbol{e}_{K,1}$$
$$\widehat{\boldsymbol{H}_K} = [\widehat{\boldsymbol{h}}_1, \widehat{\boldsymbol{h}}_2, \ldots, \widehat{\boldsymbol{h}}_K]. \tag{17}$$

Performance of those detectors (13)–(17) will be analyzed when $\boldsymbol{R}$ is estimated according to (12). In particular, performance of a detector $\boldsymbol{f}$ is measured by the average SINR

$$\mathrm{SINR}(\boldsymbol{f}) \triangleq \frac{\left|\boldsymbol{f}^H \boldsymbol{h}_1\right|^2}{\boldsymbol{f}^H \boldsymbol{R}_{\mathrm{int}} \boldsymbol{f}}, \qquad \boldsymbol{R}_{\mathrm{int}} = \boldsymbol{R} - \boldsymbol{h}_1 \boldsymbol{h}_1^H \tag{18}$$

and the analytical BER approximated by [15]

$$P_e(\boldsymbol{f}) \approx Q\left(\sqrt{\mathrm{SINR}(\boldsymbol{f})}\right) \tag{19}$$

assuming binary inputs.

III. Performance Analysis of Different Detectors

First we examine the case where there is no channel estimation error, which can be applied to a flat-fading scenario. Each $\boldsymbol{C}_j$ in (3) reduces to a code vector. We thus ignore (15). Therefore, only the DMI and subspace MMSE detectors, the subspace ZF detector, and the hybrid detector are analyzed in detail. Then we analyze all five detectors when channel $\boldsymbol{g}_j$ represents multipath fading for user j (including user 1) and is estimated from the following subspace method [20]:

$$\widehat{\boldsymbol{g}}_j = \arg\min_{\boldsymbol{g}} \boldsymbol{g}^H \boldsymbol{C}_j^H \widehat{\boldsymbol{U}}_n \widehat{\boldsymbol{U}}_n^H \boldsymbol{C}_j \boldsymbol{g}. \tag{20}$$

In general, detector $\boldsymbol{f}$ is perturbed to be $\widehat{\boldsymbol{f}} = \boldsymbol{f} + \delta\boldsymbol{f}$ where perturbation $\delta\boldsymbol{f}$ is assumed to have zero mean. According to (18), the SINR becomes

$$\widetilde{\mathrm{SINR}}(\widehat{\boldsymbol{f}}) = \frac{\boldsymbol{f}^H \boldsymbol{h}_1 \boldsymbol{h}_1^H \boldsymbol{f} + E\left\{\delta\boldsymbol{f}^H \boldsymbol{h}_1 \boldsymbol{h}_1 \delta\boldsymbol{f}\right\}}{\boldsymbol{f}^H \boldsymbol{R}_{\mathrm{int}} \boldsymbol{f} + E\left\{\delta\boldsymbol{f}^H \boldsymbol{R}_{\mathrm{int}} \delta\boldsymbol{f}\right\}} \tag{21}$$

and the analytical BER is approximated by

$$\widetilde{P_e}(\widehat{\boldsymbol{f}}) \approx Q\left(\sqrt{\widetilde{\mathrm{SINR}}(\widehat{\boldsymbol{f}})}\right). \tag{22}$$

Perturbation $\delta\boldsymbol{f}$ results from imperfect estimation of $\boldsymbol{R}$ in the current context. In our later discussion, its expression to be derived will be truncated at the first order of covariance estimation error $\delta\boldsymbol{R}$, while higher order terms are ignored. Therefore, each approximation for $\delta\boldsymbol{f}$ will be valid up to the first order of the perturbation $\delta\boldsymbol{R}$. For notationalal convenience, an approximation will be denoted by "$\approx$". It is observed that both expected values in (21) are required to obtain the $\widetilde{\mathrm{SINR}}(\widehat{\boldsymbol{f}})$. However, they follow a general form

$$\psi(\boldsymbol{X}) \triangleq E\{\delta\boldsymbol{f}^H \boldsymbol{X} \delta\boldsymbol{f}\}$$

where $\boldsymbol{X}$ can be replaced by either $\boldsymbol{h}_1\boldsymbol{h}_1^H$ or $\boldsymbol{R}_{\mathrm{int}}$. Then it suffices to derive a closed-form expression for this quantity next. Perturbation $\delta\boldsymbol{f}$ will take different forms for different detectors. To avoid being overwhelmed by derivations, we will summarize all results at the end of this section.

A. Flat Channel

In this case, we denote $\boldsymbol{C}_1$ by a vector form $\boldsymbol{c}_1$. Replacing estimated quantities explicitly by their perturbations, perturbations in detectors $\widehat{\boldsymbol{m}}_1$, $\widehat{\boldsymbol{m}}_2$, $\widehat{\boldsymbol{d}}_2$, $\widehat{\boldsymbol{w}}$ can be derived.

1) DMI MMSE Detector: According to (13), we can find

$$\delta\boldsymbol{m}_1 \approx -\boldsymbol{R}^{-1}\delta\boldsymbol{R}\boldsymbol{m}_1. \tag{23}$$

Substituting $\delta\boldsymbol{f}$ by $\delta\boldsymbol{m}_1$, we have

$$\psi(\boldsymbol{X}) = \boldsymbol{m}_1^H E\{\delta\boldsymbol{R}\boldsymbol{R}^{-1}\boldsymbol{X}\boldsymbol{R}^{-1}\delta\boldsymbol{R}\}\boldsymbol{m}_1. \tag{24}$$

Further simplification of (24) requires the second-order statistics of $\delta\boldsymbol{R}$ in a general form $\boldsymbol{\Psi}(\boldsymbol{D}) = E\{\delta\boldsymbol{R}\boldsymbol{D}\delta\boldsymbol{R}\}$ where $\boldsymbol{D}$ can be substituted by $\boldsymbol{R}^{-1}\boldsymbol{X}\boldsymbol{R}^{-1}$. It will be frequently required in subsequent analyses and has been derived in closed form in a recent work [19]. Due to its importance to our analysis, we restate the result in the following lemma.

Lemma 1 [19]: For channel input/output model (7) with inputs drawn from the same constellation, if $\widehat{\boldsymbol{R}}$ is estimated from N independent vectors by (12), then for a real-valued communication system, $\boldsymbol{\Psi}(\boldsymbol{D})$ takes the following form:

$$\begin{aligned}\boldsymbol{\Psi}(\boldsymbol{D}) = \frac{\kappa_{4b}}{N}\boldsymbol{H}[\boldsymbol{I}\odot(\boldsymbol{H}^T\boldsymbol{D}\boldsymbol{H})]\boldsymbol{H}^T \\ + \frac{1}{N}\mathrm{tr}(\boldsymbol{R}\boldsymbol{D})\boldsymbol{R} + \frac{1}{N}\boldsymbol{R}\boldsymbol{D}^T\boldsymbol{R}\end{aligned} \tag{25}$$

while for a complex-valued system, it takes a different form

$$\boldsymbol{\Psi}(\boldsymbol{D}) = \frac{\kappa_{4b}}{N}\boldsymbol{H}[\boldsymbol{I}\odot(\boldsymbol{H}^H\boldsymbol{D}\boldsymbol{H})]\boldsymbol{H}^H + \frac{1}{N}\mathrm{tr}(\boldsymbol{R}\boldsymbol{D})\boldsymbol{R} \tag{26}$$

where κ_{4b} is the fourth-order cumulant of each input, "$\odot$" represents matrix Hadamard (element-wise) product [21]. □

Differentiation by real-valued and complex-valued systems in Lemma 1 is due to different statistical properties of a real and a complex random variable. For example, for a zero-mean complex symmetric random variable x, $E\{x^2\} = 0$. But for a real random variable x, it is nonzero in general. Detailed explanation can be found in [19].

With either (25) or (26), our task becomes easier. Then (24) becomes

$$\psi(\boldsymbol{X}) = \boldsymbol{m}_1^H \boldsymbol{\Psi}(\boldsymbol{R}^{-1}\boldsymbol{X}\boldsymbol{R}^{-1})\boldsymbol{m}_1 \tag{27}$$

which is ready to evaluate since it only involves deterministic quantities. It can be observed that this quantity is inversely proportional to N, indicating that perturbations in both signal power and interference plus noise power decay roughly at a rate $\frac{1}{N}$. However, they may experience different actual decaying rates since $\boldsymbol{X}$ takes different forms as explained earlier.

2) Subspace MMSE Detector: From (14), we obtain

$$\begin{aligned}\delta\boldsymbol{m}_2 \approx \delta\boldsymbol{U}_s\boldsymbol{\Lambda}_s^{-1}\boldsymbol{U}_s^H\boldsymbol{h}_1 - \boldsymbol{U}_s\boldsymbol{\Lambda}_s^{-1}\delta\boldsymbol{\Lambda}_s\boldsymbol{\Lambda}_s^{-1}\boldsymbol{U}_s^H\boldsymbol{h}_1 \\ + \boldsymbol{U}_s\boldsymbol{\Lambda}_s^{-1}\delta\boldsymbol{U}_s^H\boldsymbol{h}_1.\end{aligned} \tag{28}$$

Perturbation $\delta\boldsymbol{R}$ causes subspace components perturbed. The results can be found in the following lemma.

Lemma 2 [18]: If $\boldsymbol{R}$ is perturbed by $\delta\boldsymbol{R}$, then its eigencomponents are perturbed by

$$\begin{aligned}\delta\boldsymbol{U}_s &\approx \boldsymbol{U}_n\boldsymbol{U}_n^H\delta\boldsymbol{R}\boldsymbol{U}_s\boldsymbol{\Omega}^{-1}, & \delta\boldsymbol{U}_n &\approx -\boldsymbol{U}_s\boldsymbol{\Omega}^{-1}\boldsymbol{U}_s^H\delta\boldsymbol{R}\boldsymbol{U}_n \\ \delta\boldsymbol{\Lambda}_s &\approx \boldsymbol{U}_s^H\delta\boldsymbol{R}\boldsymbol{U}_s, & \delta\boldsymbol{\Lambda}_n &\approx \boldsymbol{U}_n^H\delta\boldsymbol{R}\boldsymbol{U}_n.\end{aligned} \tag{29}$$

The approximation is valid up to the first order of $\delta\boldsymbol{R}$. □

Since $\boldsymbol{U}_n^H\boldsymbol{h}_1 = \boldsymbol{0}$, substituting (29) in (28) we obtain

$$\delta\boldsymbol{m}_2 \approx \boldsymbol{A}_n\delta\boldsymbol{R}\boldsymbol{A}_\gamma\boldsymbol{h}_1 - \boldsymbol{A}_s\delta\boldsymbol{R}\boldsymbol{A}_s\boldsymbol{h}_1 \tag{30}$$

where for convenience we have defined $\boldsymbol{A}_n \triangleq \boldsymbol{U}_n\boldsymbol{U}_n^H$, $\boldsymbol{A}_s \triangleq \boldsymbol{U}_s\boldsymbol{\Lambda}_s^{-1}\boldsymbol{U}_s^H$, $\boldsymbol{A}_\omega \triangleq \boldsymbol{U}_s\boldsymbol{\Omega}^{-1}\boldsymbol{U}_s^H$, $\boldsymbol{A}_\gamma \triangleq \boldsymbol{A}_s\boldsymbol{A}_\omega$. It is a function of $\delta\boldsymbol{R}$. Then $\psi(\boldsymbol{X}) = E\left\{\delta\boldsymbol{m}_2^H\boldsymbol{X}\delta\boldsymbol{m}_2\right\}$ can be derived from statistics $\boldsymbol{\Psi}(\boldsymbol{D})$ of $\delta\boldsymbol{R}$ given in Lemma 1.

3) Subspace ZF Detector: This detector is given by (16), from which its perturbation follows a form

$$\begin{aligned}\delta\boldsymbol{d}_2 \approx \delta\boldsymbol{U}_s\boldsymbol{\Omega}^{-1}\boldsymbol{U}_s^H\boldsymbol{h}_1 - \boldsymbol{U}_s\boldsymbol{\Omega}^{-1}\delta\boldsymbol{\Omega}\boldsymbol{\Omega}^{-1}\boldsymbol{U}_s^H\boldsymbol{h}_1 \\ + \boldsymbol{U}_s\boldsymbol{\Omega}^{-1}\delta\boldsymbol{U}_s^H\boldsymbol{h}_1.\end{aligned} \tag{31}$$

According to (9), $\delta\boldsymbol{\Omega} = \delta\boldsymbol{\Lambda}_s - \frac{1}{L}\mathrm{tr}(\delta\boldsymbol{\Lambda}_n)\boldsymbol{I}$ where

$$\frac{1}{L}\mathrm{tr}(\delta\boldsymbol{\Lambda}_n) = \frac{1}{L}\mathrm{tr}\left(\boldsymbol{U}_n^H\delta\boldsymbol{R}\boldsymbol{U}_n\right)$$

based on (29). After using the "vec" operation which stacks all columns of a matrix successively in a long column vector [21] to define

$$\boldsymbol{a}_n \triangleq \frac{1}{L}\mathrm{vec}\left(\boldsymbol{U}_n\boldsymbol{U}_n^H\right), \quad \delta\boldsymbol{r} \triangleq \mathrm{vec}(\delta\boldsymbol{R})$$

and applying (29), we can express $\delta\boldsymbol{\Omega}$ as

$$\delta\boldsymbol{\Omega} = \boldsymbol{U}_s^H\delta\boldsymbol{R}\boldsymbol{U}_s - (\delta\boldsymbol{r}^H\boldsymbol{a}_n)\boldsymbol{I}. \tag{32}$$

Invoking (29) once more, substituting (32) and noticing that $\boldsymbol{U}_n^H\boldsymbol{h}_1 = \boldsymbol{0}$, (31) becomes

$$\delta\boldsymbol{d}_2 \approx \boldsymbol{A}_n\delta\boldsymbol{R}\boldsymbol{A}_\omega\boldsymbol{d}_2 - \boldsymbol{A}_\omega\delta\boldsymbol{R}\boldsymbol{d}_2 + (\delta\boldsymbol{r}^H\boldsymbol{a}_n)\boldsymbol{A}_\omega\boldsymbol{d}_2. \tag{33}$$

After defining $\boldsymbol{\Phi}_r \triangleq E\{\delta\boldsymbol{r}\delta\boldsymbol{r}^H\}$ and applying the following properties [21]:

$$\begin{aligned}\mathrm{tr}(\boldsymbol{A}_1\boldsymbol{A}_2) &= \mathrm{vec}^H\left(\boldsymbol{A}_1^H\right)\mathrm{vec}(\boldsymbol{A}_2)\\ &= \mathrm{tr}(\boldsymbol{A}_2\boldsymbol{A}_1)\\ &= \mathrm{vec}^H\left(\boldsymbol{A}_2^H\right)\mathrm{vec}(\boldsymbol{A}_1)\end{aligned} \tag{34}$$

$\psi(\boldsymbol{X}) = E\left\{\delta\boldsymbol{d}_2^H\boldsymbol{X}\delta\boldsymbol{d}_2\right\}$ can be simplified as

$$\begin{aligned}\psi(\boldsymbol{X}) =& \boldsymbol{d}_2^H\boldsymbol{A}_\omega\boldsymbol{\Psi}(\boldsymbol{A}_n\boldsymbol{X}\boldsymbol{A}_n)\boldsymbol{A}_\omega\boldsymbol{d}_2 - \boldsymbol{d}_2^H\boldsymbol{A}_\omega\boldsymbol{\Psi}(\boldsymbol{A}_n\boldsymbol{X}\boldsymbol{A}_\omega)\boldsymbol{d}_2\\ &+ \mathrm{vec}^H\left(\boldsymbol{A}_\omega\boldsymbol{d}_2\boldsymbol{d}_2^H\boldsymbol{A}_\omega\boldsymbol{X}\boldsymbol{A}_n\right)\boldsymbol{\Phi}_r\boldsymbol{a}_n\\ &- \boldsymbol{d}_2^H\boldsymbol{\Psi}(\boldsymbol{A}_\omega\boldsymbol{X}\boldsymbol{A}_n)\boldsymbol{A}_\omega\boldsymbol{d}_2 + \boldsymbol{d}_2^H\boldsymbol{\Psi}(\boldsymbol{A}_\omega\boldsymbol{X}\boldsymbol{A}_\omega)\boldsymbol{d}_2\\ &- \mathrm{vec}^H\left(\boldsymbol{d}_2\boldsymbol{d}_2^H\boldsymbol{A}_\omega\boldsymbol{X}\boldsymbol{A}_\omega\right)\boldsymbol{\Phi}_r\boldsymbol{a}_n\\ &+ \boldsymbol{a}_n^H\boldsymbol{\Phi}_r\mathrm{vec}\left(\boldsymbol{A}_\omega\boldsymbol{d}_2\boldsymbol{d}_2^H\boldsymbol{A}_\omega\boldsymbol{X}\boldsymbol{A}_n\right)\\ &- \boldsymbol{a}_n^H\boldsymbol{\Phi}_r\mathrm{vec}\left(\boldsymbol{d}_2\boldsymbol{d}_2^H\boldsymbol{A}_\omega\boldsymbol{X}\boldsymbol{A}_\omega\right)\\ &+ \left(\boldsymbol{a}_n^H\boldsymbol{\Phi}_r\boldsymbol{a}_n\right)\boldsymbol{d}_2^H\boldsymbol{A}_\omega\boldsymbol{X}\boldsymbol{A}_\omega\boldsymbol{d}_2\end{aligned} \tag{35}$$

where the Hermitian property of $\boldsymbol{X}$ and other matrices has been applied. Each term on the right-hand side can be easily evaluated as long as $\boldsymbol{\Phi}_r$ is available. According to our definition, $\boldsymbol{\Phi}_r$ is the covariance of vectorized estimated data covariance. Its expression depends on the channel input/output model (7) and our covariance estimation method (12). For clarity, we provide analytical expressions for $\boldsymbol{\Phi}_r$ in the following proposition whose proof is given in Appendix.

Proposition: If a channel model follows (7) with specified dimension of $\boldsymbol{H}$ as $\nu \times \mu$, and data covariance is estimated from N independent data vectors by (12), then for a real system, the covariance of $\widehat{\boldsymbol{r}} = \mathrm{vec}(\widehat{\boldsymbol{R}})$ satisfies

$$\begin{aligned}N\boldsymbol{\Phi}_r =& \kappa_{4b}(\boldsymbol{H}\Box\boldsymbol{H})(\boldsymbol{H}\Box\boldsymbol{H})^T + \boldsymbol{R}\otimes\boldsymbol{R}\\ &+ \left[(\boldsymbol{I}_\nu\otimes\boldsymbol{1}_\nu)\boldsymbol{R}\left(\boldsymbol{1}_\nu^T\otimes\boldsymbol{I}_\nu\right)\right]\\ &\odot\left[(\boldsymbol{1}_\nu\otimes\boldsymbol{I}_\nu)\boldsymbol{R}\left(\boldsymbol{I}_\nu\otimes\boldsymbol{1}_\nu^T\right)\right]\end{aligned} \tag{36}$$

while for a complex system it satisfies

$$N\boldsymbol{\Phi}_r = \kappa_{4b}(\boldsymbol{H}^*\Box\boldsymbol{H})(\boldsymbol{H}^*\Box\boldsymbol{H})^H + \boldsymbol{R}^*\otimes\boldsymbol{R} \tag{37}$$

where "$\otimes$" stands for matrix Kronecker product, "$\Box$" for matrix Khatri–Rao product (column-wise Kronecker product) [21], "*" represents complex conjugate, $\boldsymbol{I}_\nu$ is an identity matrix of dimension ν, and $\boldsymbol{1}_\nu$ is a vector of length ν whose elements are all equal to one. □

This proposition provides a direct method to compute $\boldsymbol{\Phi}_r$ for given system parameters. It can be observed that it is also inversely proportional to N. Once it is evaluated from either (36) or (37), (35) can be easily obtained.

4) Hybrid Detector: Examination of term-by-term perturbation on (17) yields

$$\begin{aligned}\delta\boldsymbol{w} \approx& \delta\boldsymbol{U}_s\boldsymbol{\Lambda}_s^{-1}\boldsymbol{U}_s^H\boldsymbol{H}_K\boldsymbol{B}\boldsymbol{e}_{K,1}\\ &- \boldsymbol{U}_s\boldsymbol{\Lambda}_s^{-1}\delta\boldsymbol{\Lambda}_s\boldsymbol{\Lambda}_s^{-1}\boldsymbol{U}_s^H\boldsymbol{H}_K\boldsymbol{B}\boldsymbol{e}_{K,1}\\ &+ \boldsymbol{U}_s\boldsymbol{\Lambda}_s^{-1}\delta\boldsymbol{U}_s^H\boldsymbol{H}_K\boldsymbol{B}\boldsymbol{e}_{K,1}\\ &- \boldsymbol{A}_s\boldsymbol{H}_K\boldsymbol{B}\boldsymbol{H}_K^H\delta\boldsymbol{U}_s\boldsymbol{\Lambda}_s^{-1}\boldsymbol{U}_s^H\boldsymbol{H}_K\boldsymbol{B}\boldsymbol{e}_{K,1}\\ &+ \boldsymbol{A}_s\boldsymbol{H}_K\boldsymbol{B}\boldsymbol{H}_K^H\boldsymbol{U}_s\boldsymbol{\Lambda}_s^{-1}\delta\boldsymbol{\Lambda}_s\boldsymbol{\Lambda}_s^{-1}\boldsymbol{U}_s^H\boldsymbol{H}_K\boldsymbol{B}\boldsymbol{e}_{K,1}\\ &- \boldsymbol{A}_s\boldsymbol{H}_K\boldsymbol{B}\boldsymbol{H}_K^H\boldsymbol{U}_s\boldsymbol{\Lambda}_s^{-1}\delta\boldsymbol{U}_s^H\boldsymbol{H}_K\boldsymbol{B}\boldsymbol{e}_{K,1}\end{aligned} \tag{38}$$

where for shorter notation we have defined

$$\boldsymbol{B} \triangleq \left(\boldsymbol{H}_K^H\boldsymbol{U}_s\boldsymbol{\Lambda}_s^{-1}\boldsymbol{U}_s^H\boldsymbol{H}_K\right)^{-1}.$$

After applying (29) and noticing $\boldsymbol{U}_n^H\boldsymbol{H}_K = \boldsymbol{0}$, (38) becomes

$$\begin{aligned}\delta\boldsymbol{w} \approx& \boldsymbol{A}_n\delta\boldsymbol{R}\boldsymbol{A}_\omega\boldsymbol{w} - \boldsymbol{A}_s\delta\boldsymbol{R}\boldsymbol{w} - \boldsymbol{A}_s\boldsymbol{H}_K\boldsymbol{B}\boldsymbol{H}_K^H\boldsymbol{A}_n\delta\boldsymbol{R}\boldsymbol{A}_\omega\boldsymbol{w}\\ &+\boldsymbol{A}_s\boldsymbol{H}_K\boldsymbol{B}\boldsymbol{H}_K^H\boldsymbol{A}_s\delta\boldsymbol{R}\boldsymbol{w}.\end{aligned} \tag{39}$$

This shows a relation of $\delta\boldsymbol{w}$ to $\delta\boldsymbol{R}$. Thus,

$$\psi(\boldsymbol{X}) = E\left\{\delta\boldsymbol{w}^H\boldsymbol{X}\delta\boldsymbol{w}\right\}$$

can be evaluated similarly as before from the second-order statistics of the covariance estimate given in Lemma 1. A detailed expression is omitted for brevity. In our later discussion, we will adopt the same strategy for the same reason when perturbation $\delta\boldsymbol{f}$ of detector $\boldsymbol{f}$ has a long expression. If it is a function of $\delta\boldsymbol{R}$ only, then direct application of results in Lemma 1 is sufficient. If it is a function of both $\delta\boldsymbol{R}$ and $\delta\boldsymbol{r}$, then $E\{\delta\boldsymbol{f}^H\boldsymbol{X}\delta\boldsymbol{f}\}$ involves the second order statistics of $\delta\boldsymbol{R}$, $\delta\boldsymbol{r}$, and cross correlation between $\delta\boldsymbol{R}$ and $\delta\boldsymbol{r}$. The last one can be easily converted into a typical form $E\{\boldsymbol{x}^H\delta\boldsymbol{R}\boldsymbol{X}\delta\boldsymbol{r}\}$. After applying properties (34) and the following [21]:

$$\begin{aligned}\mathrm{vec}(\boldsymbol{A}_1\boldsymbol{A}_2\boldsymbol{A}_3) &= \left(\boldsymbol{A}_3^T\otimes\boldsymbol{A}_1\right)\mathrm{vec}(\boldsymbol{A}_2)\\ (\boldsymbol{A}_1\otimes\boldsymbol{A}_2)^T &= \boldsymbol{A}_1^T\otimes\boldsymbol{A}_2^T\end{aligned}$$

it becomes

$$E\{\boldsymbol{x}^H\delta\boldsymbol{R}\boldsymbol{X}\delta\boldsymbol{r}\} = \mathrm{tr}((\boldsymbol{x}^*\otimes\boldsymbol{X})\boldsymbol{\Phi}_r). \tag{40}$$

It can thus be evaluated using our results for $\boldsymbol{\Phi}_r$ in the *Proposition*.

So far, we have derived analytical expressions for $\psi(\boldsymbol{X})$ for each of the four detectors which lead to direct evaluation of their analytical SINRs and BERs. Though performance comparison among different detectors turns out to be much involved for a fixed N, we mainly rely on simulation study later and meanwhile verify all analytical results therein.

B. Multipath Channel

When a multipath channel is present, $\boldsymbol{g}_j$ can be estimated first by (20) and then different detectors are constructed. The analysis is more complicated since each estimated channel vector is also perturbed to be $\widehat{\boldsymbol{g}}_j = \boldsymbol{g}_j + \delta\boldsymbol{g}_j$ with perturbation $\delta\boldsymbol{g}_j$. Let us first derive $\delta\boldsymbol{g}_j$ due to $\delta\boldsymbol{R}$.

For convenience, denote the unperturbed objective matrix in (20) by $\boldsymbol{O}_j \triangleq \boldsymbol{C}_j^H\boldsymbol{U}_n\boldsymbol{U}_n^H\boldsymbol{C}_j$. Since $\boldsymbol{R}$ is perturbed by $\delta\boldsymbol{R}$, its noise subspace shows a perturbation as $\delta\boldsymbol{U}_n \approx -\boldsymbol{A}_\omega\delta\boldsymbol{R}\boldsymbol{U}_n$ according to Lemma 2. Such a perturbation causes $\boldsymbol{O}_j$ perturbed with perturbation

$$\delta\boldsymbol{O}_j \approx \boldsymbol{C}_j^H\delta\boldsymbol{U}_n\boldsymbol{U}_n^H\boldsymbol{C}_j + \boldsymbol{C}_j^H\boldsymbol{U}_n\delta\boldsymbol{U}_n^H\boldsymbol{C}_j.$$

Since $\boldsymbol{g}_j$ is the minimum eigenvector of $\boldsymbol{O}_j$, $\delta\boldsymbol{g}_j$ can be found to be $\delta\boldsymbol{g}_j \approx -\boldsymbol{O}_j^\dagger\delta\boldsymbol{O}_j\boldsymbol{g}_j$. Noticing that $\boldsymbol{U}_n^H\boldsymbol{C}_j\boldsymbol{g}_j = \boldsymbol{0}$, $\delta\boldsymbol{g}_j$ is finally related to $\delta\boldsymbol{R}$ by

$$\delta\boldsymbol{g}_j \approx \boldsymbol{O}_j^\dagger\boldsymbol{C}_j^H\boldsymbol{A}_n\delta\boldsymbol{R}\boldsymbol{A}_\omega\boldsymbol{h}_j. \tag{41}$$

With this clear relation, we are ready to evaluate previously presented different detectors. We will follow similar procedures as before, but incorporate (41). The typical term in the expression of SINR is still

$$\psi(\boldsymbol{X}) = E\left\{\delta\boldsymbol{f}^H\boldsymbol{X}\delta\boldsymbol{f}\right\}$$

where $\boldsymbol{X}$ can be replaced by either $\boldsymbol{h}_1\boldsymbol{h}_1^H$ or $\boldsymbol{R}_{\text{int}}$.

1) DMI MMSE Detector: According to (13), we can find

$$\delta\boldsymbol{m}_1 \approx -\boldsymbol{R}^{-1}\delta\boldsymbol{R}\boldsymbol{m}_1 + \boldsymbol{R}^{-1}\boldsymbol{C}_1\delta\boldsymbol{g}_1. \tag{42}$$

Compared with (23), an additional term appears due to channel estimation error. Thus, more terms are expected in our final expression for $\psi(\boldsymbol{X})$. Readers will easily find similar situations in our later discussions on other detectors. Using (41), (42) becomes

$$\delta\boldsymbol{m}_1 \approx -\boldsymbol{R}^{-1}\delta\boldsymbol{R}\boldsymbol{m}_1 + \boldsymbol{R}^{-1}\boldsymbol{Q}_1\boldsymbol{A}_n\delta\boldsymbol{R}\boldsymbol{d}_2 \tag{43}$$

where $\boldsymbol{Q}_j \triangleq \boldsymbol{C}_j\boldsymbol{O}_j^\dagger\boldsymbol{C}_j^H$ for all j's including $j=1$. It is a function of $\delta\boldsymbol{R}$. Then $E\left\{\delta\boldsymbol{f}^H\boldsymbol{X}\delta\boldsymbol{f}\right\}$ easily follows.

2) Subspace MMSE Detector: From (14), we obtain

$$\begin{aligned}\delta\boldsymbol{m}_2 \approx{}& \delta\boldsymbol{U}_s\boldsymbol{\Lambda}_s^{-1}\boldsymbol{U}_s^H\boldsymbol{h}_1 - \boldsymbol{U}_s\boldsymbol{\Lambda}_s^{-1}\delta\boldsymbol{\Lambda}_s\boldsymbol{\Lambda}_s^{-1}\boldsymbol{U}_s^H\boldsymbol{h}_1\\ &+\boldsymbol{U}_s\boldsymbol{\Lambda}_s^{-1}\delta\boldsymbol{U}_s^H\boldsymbol{h}_1 + \boldsymbol{A}_s\boldsymbol{C}_1\delta\boldsymbol{g}_1.\end{aligned} \tag{44}$$

After substituting (29) and (41) in (44), and noticing that $\boldsymbol{U}_n^H\boldsymbol{h}_1 = \boldsymbol{0}$, we obtain

$$\delta\boldsymbol{m}_2 \approx \boldsymbol{A}_n\delta\boldsymbol{R}\boldsymbol{A}_\gamma\boldsymbol{h}_1 - \boldsymbol{A}_s\delta\boldsymbol{R}\boldsymbol{m}_2 + \boldsymbol{A}_s\boldsymbol{Q}_1\boldsymbol{A}_n\delta\boldsymbol{R}\boldsymbol{d}_2. \tag{45}$$

Then $\psi(\boldsymbol{X}) = E\left\{\delta\boldsymbol{m}_2^H\boldsymbol{X}\delta\boldsymbol{m}_2\right\}$ can be obtained by straightforward substitution.

3) Direct ZF Detector: Considering a perturbation to $\boldsymbol{H}$ due to channel estimation errors for all users, perturbation in direct ZF detector (15) is given by

$$\begin{aligned}\delta\boldsymbol{d}_1 ={}& \boldsymbol{\Pi}_H^\perp\delta\boldsymbol{H}(\boldsymbol{H}^H\boldsymbol{H})^{-1}\boldsymbol{e}_{J,1}\\ &-\boldsymbol{H}(\boldsymbol{H}^H\boldsymbol{H})^{-1}\delta\boldsymbol{H}^H\boldsymbol{H}(\boldsymbol{H}^H\boldsymbol{H})^{-1}\boldsymbol{e}_{J,1}\end{aligned} \tag{46}$$

where $\boldsymbol{\Pi}_H^\perp \triangleq \boldsymbol{I} - \boldsymbol{H}(\boldsymbol{H}^H\boldsymbol{H})^{-1}\boldsymbol{H}^H$. Due to (41), $\delta\boldsymbol{H}$ is related to $\delta\boldsymbol{R}$ by

$$\delta\boldsymbol{H} = \sum_{j=1}^{J}\boldsymbol{C}_j\delta\boldsymbol{g}_j\boldsymbol{e}_{J,j}^T = \sum_{j=1}^{J}\boldsymbol{Q}_j\boldsymbol{A}_n\delta\boldsymbol{R}\boldsymbol{A}_\omega\boldsymbol{h}_j\boldsymbol{e}_{J,j}^T. \tag{47}$$

Substituting (47), (46) becomes

$$\begin{aligned}\delta\boldsymbol{d}_1 ={}& \sum_{j=1}^{J}\alpha_j\boldsymbol{\Pi}_H^\perp\boldsymbol{Q}_j\boldsymbol{A}_n\delta\boldsymbol{R}\boldsymbol{A}_\omega\boldsymbol{h}_j\\ &-\sum_{j=1}^{J}\left(\boldsymbol{h}_j^H\boldsymbol{A}_\omega\delta\boldsymbol{R}\boldsymbol{A}_n\boldsymbol{Q}_j\boldsymbol{d}_1\right)\boldsymbol{H}(\boldsymbol{H}^H\boldsymbol{H})^{-1}\boldsymbol{e}_{J,j}\end{aligned} \tag{48}$$

where $\alpha_j = \boldsymbol{e}_{J,j}^T(\boldsymbol{H}^H\boldsymbol{H})^{-1}\boldsymbol{e}_{J,1}$. It is a function of $\delta\boldsymbol{R}$. The required term $\psi(\boldsymbol{X}) = E\{\delta\boldsymbol{d}_1^H\boldsymbol{X}\delta\boldsymbol{d}_1\}$ can be easily derived.

4) Subspace ZF Detector: This detector is given by (16) which is a perturbed version of $\boldsymbol{d}_2 = \boldsymbol{A}_\omega\boldsymbol{h}_1$. The perturbation follows a form

$$\begin{aligned}\delta\boldsymbol{d}_2 \approx{}& \delta\boldsymbol{U}_s\boldsymbol{\Omega}^{-1}\boldsymbol{U}_s^H\boldsymbol{h}_1 - \boldsymbol{U}_s\boldsymbol{\Omega}^{-1}\delta\boldsymbol{\Omega}\boldsymbol{\Omega}^{-1}\boldsymbol{U}_s^H\boldsymbol{h}_1\\ &+\boldsymbol{U}_s\boldsymbol{\Omega}^{-1}\delta\boldsymbol{U}_s^H\boldsymbol{h}_1 + \boldsymbol{A}_\omega\boldsymbol{C}_1\delta\boldsymbol{g}_1.\end{aligned} \tag{49}$$

Similar to obtaining (33), (49) can be simplified as

$$\begin{aligned}\delta\boldsymbol{d}_2 \approx{}& \boldsymbol{A}_n\delta\boldsymbol{R}\boldsymbol{A}_\omega\boldsymbol{d}_2 - \boldsymbol{A}_\omega\delta\boldsymbol{R}\boldsymbol{d}_2\\ &+(\delta\boldsymbol{r}^H\boldsymbol{a}_n)\boldsymbol{A}_\omega\boldsymbol{d}_2 + \boldsymbol{A}_\omega\boldsymbol{Q}_1\boldsymbol{A}_n\delta\boldsymbol{R}\boldsymbol{d}_2.\end{aligned} \tag{50}$$

It is a function of both $\delta\boldsymbol{R}$ and $\delta\boldsymbol{r}$, similar to (33). According to our previous discussion, $\psi(\boldsymbol{X}) = E\{\delta\boldsymbol{d}_2^H\boldsymbol{X}\delta\boldsymbol{d}_2\}$ can also be similarly obtained.

5) Hybrid Detector: In (17), not only subspace components of $\boldsymbol{R}$ are perturbed, but also $\boldsymbol{H}_K$. Similar to (47), we obtain a perturbation in $\boldsymbol{H}_K$ as

$$\delta\boldsymbol{H}_K = \sum_{k=1}^{K}\boldsymbol{Q}_k\boldsymbol{A}_n\delta\boldsymbol{R}\boldsymbol{A}_\omega\boldsymbol{h}_k\boldsymbol{e}_{K,k}^T. \tag{51}$$

To simplify derivation procedures, let us first find $\delta\boldsymbol{B}$, the perturbation in the middle matrix $\boldsymbol{B}$. Considering all possible perturbation sources in $\boldsymbol{B}$, we obtain

$$\begin{aligned}\delta\boldsymbol{B} \approx{}& -\boldsymbol{B}\delta\boldsymbol{H}_K^H\boldsymbol{A}_s\boldsymbol{H}_K\boldsymbol{B} - \boldsymbol{B}\boldsymbol{H}_K^H\boldsymbol{A}_s\delta\boldsymbol{H}_K\boldsymbol{B}\\ &-\boldsymbol{B}\boldsymbol{H}_K^H\Big(\delta\boldsymbol{U}_s\boldsymbol{\Lambda}_s^{-1}\boldsymbol{U}_s^H - \boldsymbol{U}_s\boldsymbol{\Lambda}_s^{-1}\delta\boldsymbol{\Lambda}_s\boldsymbol{\Lambda}_s^{-1}\boldsymbol{U}_s^H\\ &\qquad+\boldsymbol{U}_s\boldsymbol{\Lambda}_s^{-1}\delta\boldsymbol{U}_s^H\Big)\boldsymbol{H}_K\boldsymbol{B}.\end{aligned} \tag{52}$$

Applying (29) and (51), and noticing $\boldsymbol{U}_n^H\boldsymbol{H}_K = \boldsymbol{0}$, $\delta\boldsymbol{B}$ is simplified to

$$\begin{aligned}\delta\boldsymbol{B} \approx{}& -\sum_{k=1}^{K}\boldsymbol{B}\boldsymbol{e}_{K,k}\boldsymbol{h}_k^H\boldsymbol{A}_\omega\delta\boldsymbol{R}\boldsymbol{A}_n\boldsymbol{Q}_k\boldsymbol{A}_s\boldsymbol{H}_K\boldsymbol{B}\\ &-\sum_{k=1}^{K}\boldsymbol{B}\boldsymbol{H}_K^H\boldsymbol{A}_s\boldsymbol{Q}_k\boldsymbol{A}_n\delta\boldsymbol{R}\boldsymbol{A}_\omega\boldsymbol{h}_k\boldsymbol{e}_{K,k}^T\boldsymbol{B}\\ &+\boldsymbol{B}\boldsymbol{H}_K^H\boldsymbol{A}_s\delta\boldsymbol{R}\boldsymbol{A}_s\boldsymbol{H}_K\boldsymbol{B}.\end{aligned} \tag{53}$$

According to (17), perturbation in $\boldsymbol{w}$ becomes

$$\begin{aligned}\delta\boldsymbol{w} \approx{}& \delta\boldsymbol{U}_s\boldsymbol{\Lambda}_s^{-1}\boldsymbol{U}_s^H\boldsymbol{H}_K\boldsymbol{B}\boldsymbol{e}_{K,1}\\ &-\boldsymbol{U}_s\boldsymbol{\Lambda}_s^{-1}\delta\boldsymbol{\Lambda}_s\boldsymbol{\Lambda}_s^{-1}\boldsymbol{U}_s^H\boldsymbol{H}_K\boldsymbol{B}\boldsymbol{e}_{K,1}\\ &+\boldsymbol{U}_s\boldsymbol{\Lambda}_s^{-1}\delta\boldsymbol{U}_s^H\boldsymbol{H}_K\boldsymbol{B}\boldsymbol{e}_{K,1}\\ &+\boldsymbol{A}_s\delta\boldsymbol{H}_K\boldsymbol{B}\boldsymbol{e}_{K,1} + \boldsymbol{A}_s\boldsymbol{H}_K\delta\boldsymbol{B}\boldsymbol{e}_{K,1}.\end{aligned} \tag{54}$$

Substituting (51), (53), and (29) in (54), $\delta \boldsymbol{w}$ is related to $\delta \boldsymbol{R}$ by

$$\begin{aligned}\delta \boldsymbol{w} \approx\; & \boldsymbol{A}_n \delta \boldsymbol{R} \boldsymbol{A}_\omega \boldsymbol{w} - \boldsymbol{A}_s \delta \boldsymbol{R} \boldsymbol{w} \\ & + \sum_{k=1}^{K} \beta_k \boldsymbol{A}_s \boldsymbol{Q}_k \boldsymbol{A}_n \delta \boldsymbol{R} \boldsymbol{A}_\omega \boldsymbol{h}_k \\ & - \sum_{k=1}^{K} \boldsymbol{A}_s \boldsymbol{H}_K \boldsymbol{B} \boldsymbol{e}_{K,k} \boldsymbol{h}_k^H \boldsymbol{A}_\omega \delta \boldsymbol{R} \boldsymbol{A}_n \boldsymbol{Q}_k \boldsymbol{w} \\ & - \sum_{k=1}^{K} \beta_k \boldsymbol{A}_s \boldsymbol{H}_K \boldsymbol{B} \boldsymbol{H}_K^H \boldsymbol{A}_s \boldsymbol{Q}_k \boldsymbol{A}_n \delta \boldsymbol{R} \boldsymbol{A}_\omega \boldsymbol{h}_k \\ & + \boldsymbol{A}_s \boldsymbol{H}_K \boldsymbol{B} \boldsymbol{H}_K^H \boldsymbol{A}_s \delta \boldsymbol{R} \boldsymbol{w} \end{aligned} \quad (55)$$

where $\boldsymbol{A}_s \boldsymbol{H}_K \boldsymbol{B} \boldsymbol{e}_{K,1}$ has been substituted by $\boldsymbol{w}$

$$\beta_k \triangleq \boldsymbol{e}_{K,k}^T \boldsymbol{B} \boldsymbol{e}_{K,1}.$$

It is a function of $\delta \boldsymbol{R}$. Then $\psi(\boldsymbol{X}) = E\left\{\delta \boldsymbol{w}^H \boldsymbol{X} \delta \boldsymbol{w}\right\}$ can be evaluated.

C. A Brief Summary

As observed from the expression of $\widetilde{\mathrm{SINR}}(\widehat{\boldsymbol{f}})$ in (21), $\psi(\boldsymbol{X}) = E\{\delta \boldsymbol{f}^H \boldsymbol{X} \delta \boldsymbol{f}\}$ with $\boldsymbol{X} = \boldsymbol{h}_1 \boldsymbol{h}_1^H$ contributes to the perturbation of the desired signal power, and $\psi(\boldsymbol{X})$ with $\boldsymbol{X} = \boldsymbol{R}_{\text{int}}$ contributes to the perturbation of the interference-plus-noise power. For clarity, we summarize all perturbed detectors in Table I for flat channels and in Table II for estimated multipath channels. It has been shown that each $\delta \boldsymbol{f}$ is a linear function of $\delta \boldsymbol{R}$, or $\delta \boldsymbol{r}$, or linear combination of both. Then $\psi(\boldsymbol{X})$ involves a form of either $\boldsymbol{\Psi}(\boldsymbol{D})$ by (25) or (26) in Lemma 1, or $\boldsymbol{\Phi}_r$ by (36) or (37) in our *Proposition*, or $E\{\boldsymbol{x}^H \delta \boldsymbol{R} \boldsymbol{X} \delta \boldsymbol{r}\}$ by (40) where $\boldsymbol{D}$, $\boldsymbol{x}$ and $\boldsymbol{X}$ are nominal matrices/vector, and should be replaced by the corresponding arguments, respectively. For quick reference, some quantities defined before are listed in Table III. With all those results, the corresponding terms of $\widetilde{\mathrm{SINR}}(\widehat{\boldsymbol{f}})$ in (21) can be easily obtained. Then the BER can be calculated by (22). Although each expression involves many terms and further simplification is intractable, for large N, perturbation of the desired signal power is less severe than that to the interference-plus-noise, according to our simulation study. Therefore, the output SINR (thus, BER) with finite data samples is largely affected by the variation of interference and noise power.

IV. Numerical Results

We verify all analytical results by computer simulation. The average SINR of each detector over 500 independent realizations is used as a performance measure. For concise presentation, corresponding BER will not be presented except for one case as an example. Both flat channels and multipath channels are considered. For flat channels, the analytical results for the DMI MMSE, subspace MMSE, and hybrid detectors in [15] which are based on the asymptotic limit theorem (denoted as ALT for short) are also included in order to make comparisons with those from proposed (perturbation based) analysis. Results for the subspace ZF detector are obtained from the proposed analysis. For multipath channels, all users' channel parameters are estimated by the subspace technique. Then five detectors:

TABLE I
Analytical Results for Different Detectors With Flat Channels

Blind detector	Ideal $\boldsymbol{f}$	Perturbed $\widehat{\boldsymbol{f}}$	Perturbation $\delta\boldsymbol{f}$
DMI MMSE	(4)	(13)	(23)
Subspace MMSE	(6)	(14)	(30)
Subspace ZF	(9)	(16)	(33)
Hybrid	(11)	(17)	(39)

TABLE II
Analytical Results for Different Detectors With Estimated Multipath Channels

Blind detector	Ideal $\boldsymbol{f}$	Perturbed $\widehat{\boldsymbol{f}}$	Perturbation $\delta\boldsymbol{f}$
DMI MMSE	(4)	(13)	(43)
Subspace MMSE	(6)	(14)	(45)
Direct ZF	(8)	(15)	(48)
Subspace ZF	(9)	(16)	(50)
Hybrid	(11)	(17)	(55)

TABLE III
Some Defined Quantities

$\boldsymbol{H} \triangleq [\boldsymbol{h}_1, \cdots, \boldsymbol{h}_J]$, $\boldsymbol{H}_K \triangleq [\boldsymbol{h}_1, \cdots, \boldsymbol{h}_K]$, $\boldsymbol{R}_{int} \triangleq \boldsymbol{R} - \boldsymbol{h}_1 \boldsymbol{h}_1^H$,
$\boldsymbol{A}_n \triangleq \boldsymbol{U}_n \boldsymbol{U}_n^H$, $\boldsymbol{A}_s \triangleq \boldsymbol{U}_s \boldsymbol{\Lambda}_s^{-1} \boldsymbol{U}_s^H$,
$\boldsymbol{A}_\omega \triangleq \boldsymbol{U}_s \boldsymbol{\Omega}^{-1} \boldsymbol{U}_s^H$, $\boldsymbol{A}_\gamma \triangleq \boldsymbol{A}_s \boldsymbol{A}_\omega$,
$\boldsymbol{B} \triangleq (\boldsymbol{H}_K^H \boldsymbol{U}_s \boldsymbol{\Lambda}_s^{-1} \boldsymbol{U}_s^H \boldsymbol{H}_K)^{-1}$, $\boldsymbol{O}_j \triangleq \boldsymbol{C}_j^H \boldsymbol{U}_n \boldsymbol{U}_n^H \boldsymbol{C}_j$,
$\boldsymbol{Q}_j \triangleq \boldsymbol{C}_j \boldsymbol{O}_j^\dagger \boldsymbol{C}_j^H$, $\boldsymbol{\Pi}_H^\perp \triangleq \boldsymbol{I} - \boldsymbol{H}(\boldsymbol{H}^H \boldsymbol{H})^{-1} \boldsymbol{H}^H$,
$\boldsymbol{a}_n \triangleq \frac{1}{L} vec(\boldsymbol{U}_n \boldsymbol{U}_n^H)$, L is the rank of $\boldsymbol{U}_n$,
$\alpha_j \triangleq \boldsymbol{e}_{J,j}^T (\boldsymbol{H}^H \boldsymbol{H})^{-1} \boldsymbol{e}_{J,1}$ $(j = 1, \cdots, J)$,
$\beta_k \triangleq \boldsymbol{e}_{K,k}^T \boldsymbol{B} \boldsymbol{e}_{K,1}$ $(k = 1, \cdots, K)$.

DMI MMSE, subspace MMSE, direct ZF, subspace ZF, and hybrid detectors are discussed. Effects of key parameters as the sample size, SNR, and number of users are studied as follows.

A. Flat Channel

When the communication channel is flat fading, signature waveform of the desired user is assumed known. Performance of the DMI MMSE detector explicitly depends on the accuracy of the estimated data correlation matrix, while performance of the subspace MMSE, subspace ZF and hybrid detectors depends on the accuracy of the eigencomponents of the data correlation matrix. The estimation error is primarily determined by the sample size N. Fig. 1 shows its effect on the SINR and Fig. 2 on the BER when Gold sequences of length $M = 31$ are used for all $J = 25$ users in a system with SNR= 10 dB, among which spreading codes of $K = 10$ users are assumed known in building hybrid detectors. Solid lines represent the experimental results, dash-dotted lines from our analysis, and dashed lines from ALT in [15]. The analytical BERs are approximated by (22) using corresponding analytical SINRs. From these figures, convergence of experimental results to analytical results within 1000 signal samples is observed. Secondly, analytical results based on either proposed perturbation technique or ALT agree with each other and are almost indistinguishable in the figures. Also, different detectors tend to show a similar convergence level in terms of either SINR or BER with the current system parameters. To minimize redundancy in later presentation, we will omit BER results. The effect of noise is also studied. SINRs with $N = 400$ signal samples are presented in Fig. 3 for a large range of SNRs. It is seen that the subspace

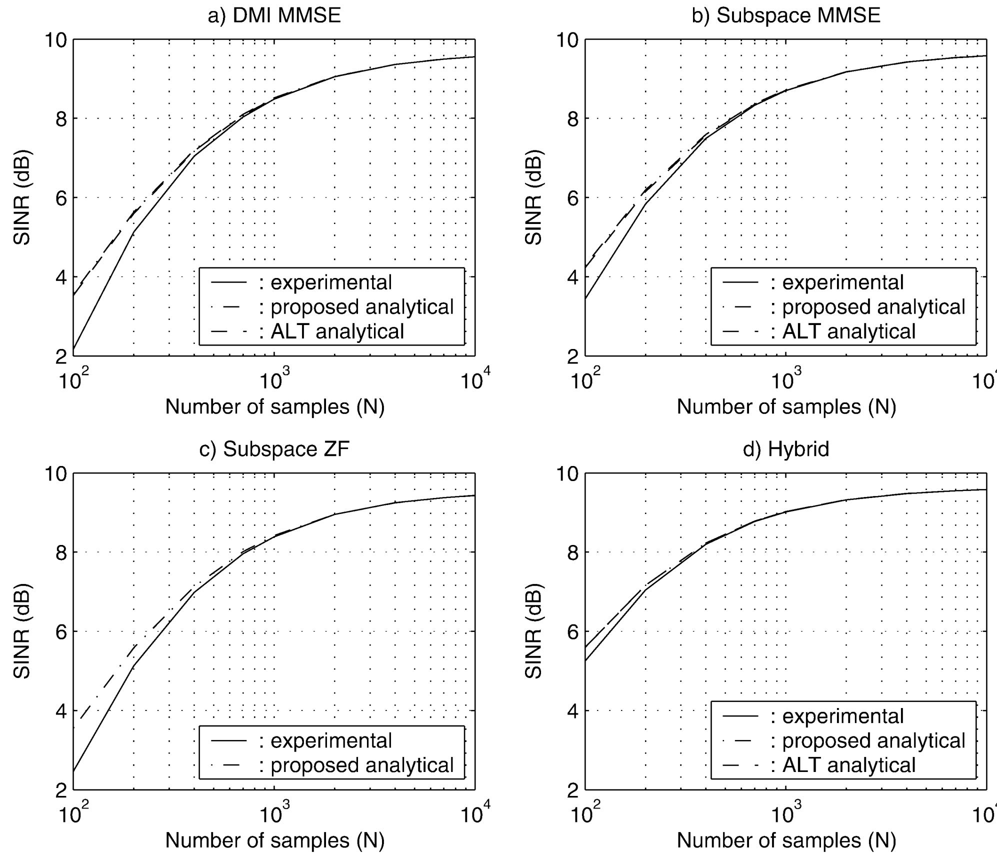

Fig. 1. The average output SINR versus the number of signal samples N for the DMI MMSE, subspace MMSE, subspace ZF, and hybrid detectors in flat channels. $M = 31$, $J = 25$, $K = 10$, SNR= 10 dB.

MMSE detector performs better than the DMI MMSE detector when SNR is high, as analyzed in [15]. It shows similar performance as the subspace ZF detector. However, the hybrid detector outperforms both the subspace MMSE and subspace ZF detectors since it zero-forces contribution of some of the interfering users. The number of users J affects the interference level and thus the performance of detectors. Fig. 4 clearly demonstrates how sensitive is their performance to J for systems with 15-dB noise, three users of known waveforms, and 400 received signal samples. Performance of all detectors degrades with increased J except the DMI detector whose performance is relatively steady but worse than other detectors for all examined J, as observed and explained in [15]. The hybrid detector still performs best. The other two detectors show similar performance. Again, analytical results highly conform to experimental results.

B. Multipath Channel

In a multipath environment, the detector's performance is affected by not only multiuser interference, but also channel distortion. In the simulation, channel of each user has four paths whose coefficients are randomly generated with equal power according to Gaussian distribution. Channel parameters for all users are estimated using the subspace technique. For comparison with both analytical results and performance of other detectors, direct ZF detectors are also inclusively studied. Therefore, in total, five detectors are compared in each experiment. Fig. 5 plots the SINR versus the number of signal samples when there are $J = 15$ users in a 15-dB CDMA system. In building the direct ZF detector, all users' channels are estimated, while in building the hybrid detector, channels of $K = 10$ users are estimated. For all other detectors, only the desired user's channel is estimated. It can be seen that all analytical results are consistent with the corresponding experimental results for large N. The performance of the direct ZF detector is less sensitive to all examined N (currently above 100) since this detector does not use estimated data covariance directly whose accuracy heavily relies on the sample size. It directly uses estimated channels which are satisfactory even for relatively small N. All other detectors exhibit improved performance as N increases and similar convergence level after 10^4 samples are processed. The hybrid detector shows better performance for small number of samples than all other detectors except the direct ZF detector. Fig. 6 presents performance with respect to different SNRs when $N = 200$ samples are processed. It is clear that the direct ZF detector performs best for moderate to high SNRs, followed by the hybrid detector. The subspace ZF and subspace MMSE detectors show similar performance, and are better than the DMI MMSE detector since the noise effect may be enhanced in the latter. The effect of the system load is further studied in Fig. 7. When the load is moderate, the direct ZF detector outperforms all others. With increased load, errors from estimating all users' channels significantly degrade its performance. However, for the hybrid detector, since the number of known users is small and estimation errors only affect the performance moderately. This detector performs best for a large range of J. Subspace ZF and

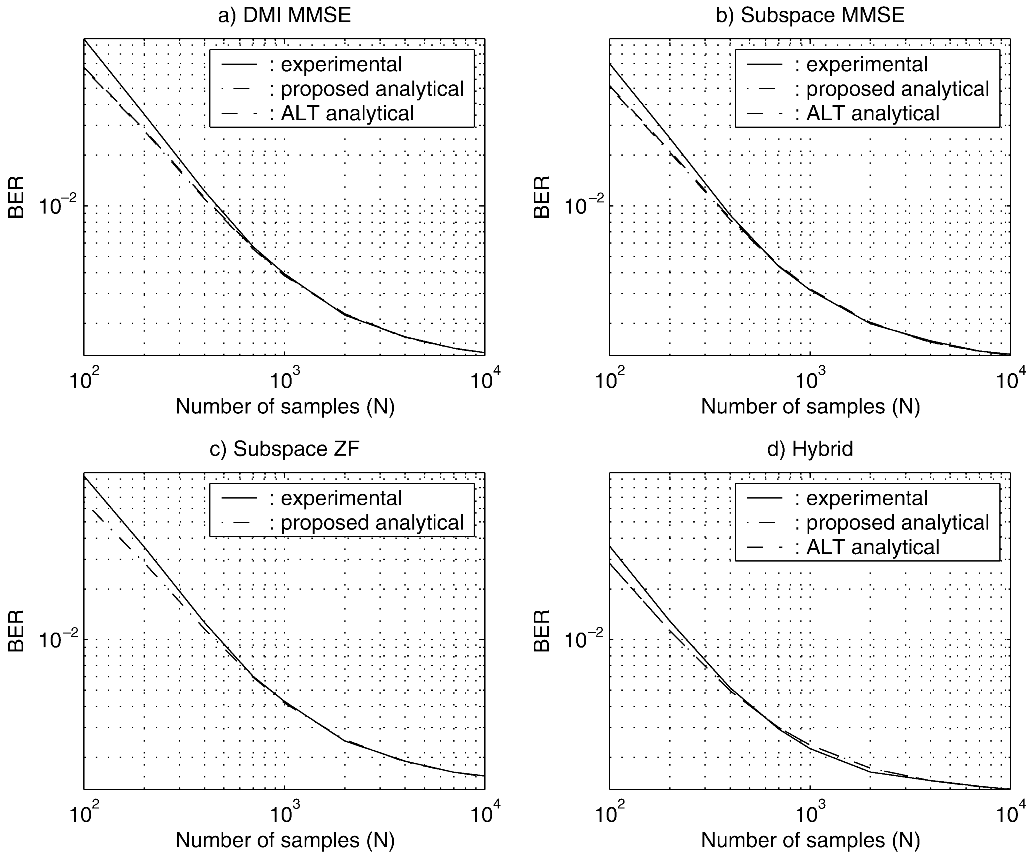

Fig. 2. The average BER versus the number of signal samples N for the DMI MMSE, subspace MMSE, subspace ZF, and hybrid detectors in flat channels. $M = 31$, $J = 25$, $K = 10$, SNR= 10 dB.

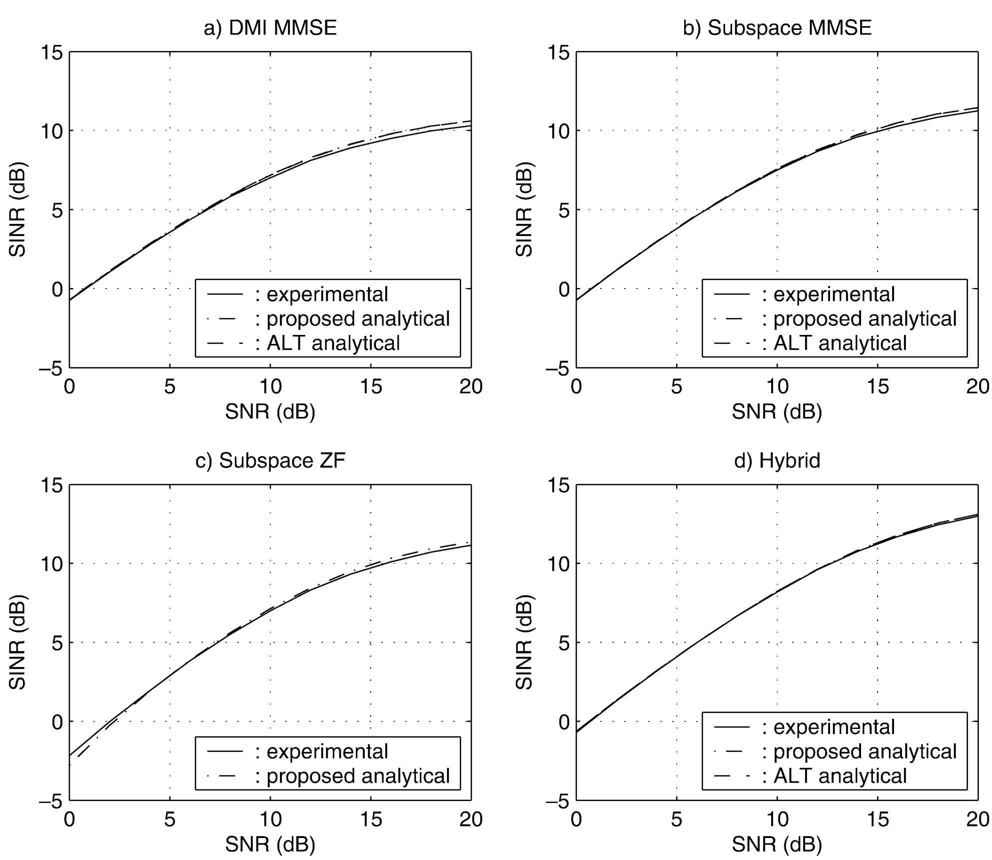

Fig. 3. The average output SINR versus SNR for the DMI MMSE, subspace MMSE, subspace ZF, and hybrid detectors in flat channels. $M = 31$, $J = 25$, $K = 10$, $N = 400$.

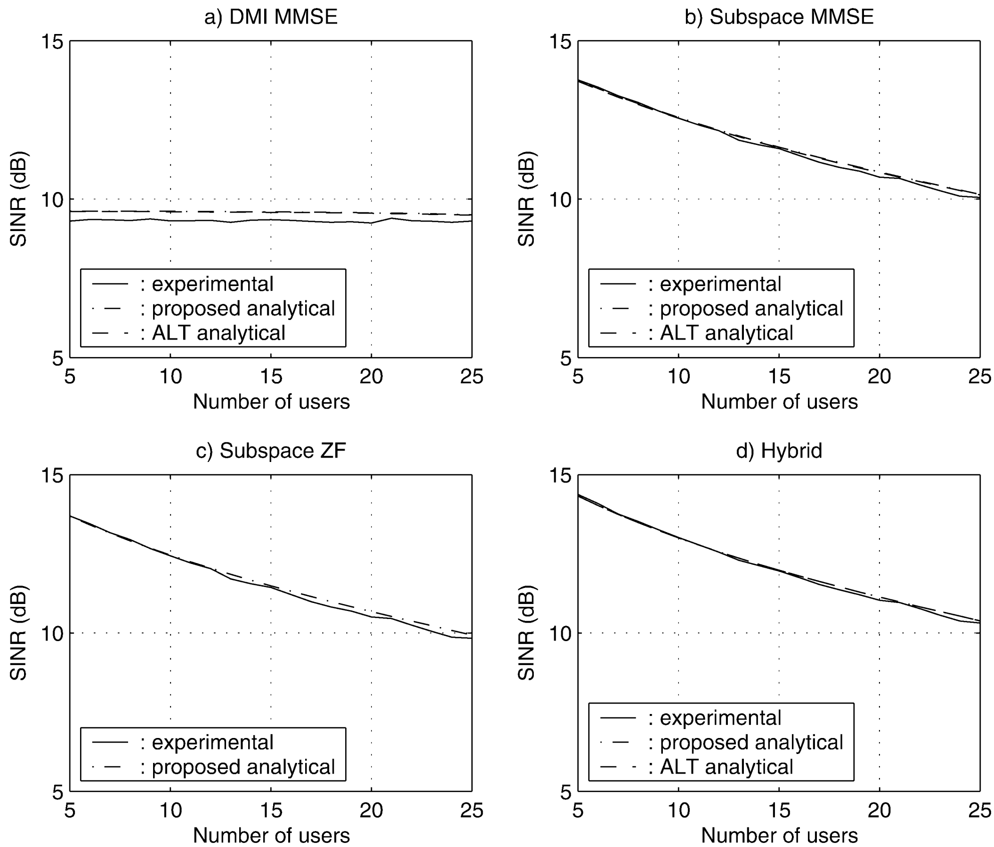

Fig. 4. The average output SINR versus the number of users for the DMI MMSE, subspace MMSE, subspace ZF, and hybrid detectors in flat channels. $M = 31$, $K = 3$, SNR= 15 dB, $N = 400$.

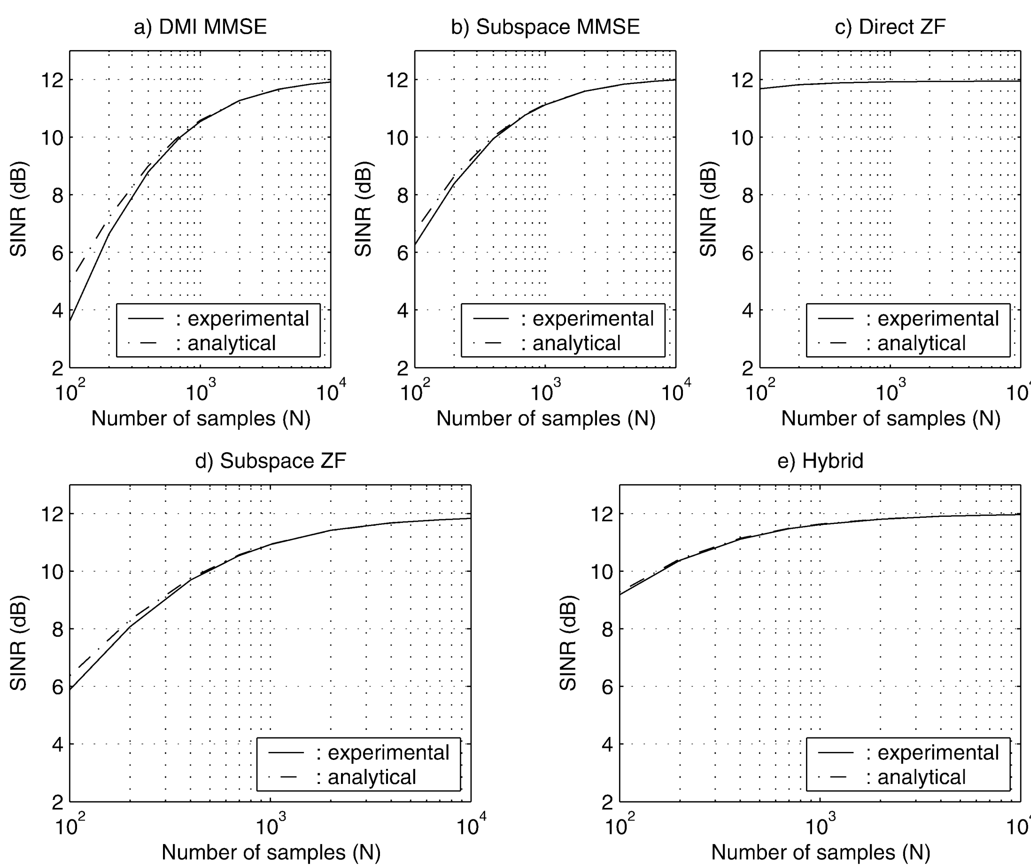

Fig. 5. The average output SINR versus the number of signal samples N for the DMI MMSE, subspace MMSE, direct ZF, subspace ZF, and hybrid detectors in multipath channels. Channel parameters are estimated by the subspace method. $M = 31, q = 3, J = 15, K = 10$, SNR= 15 dB.

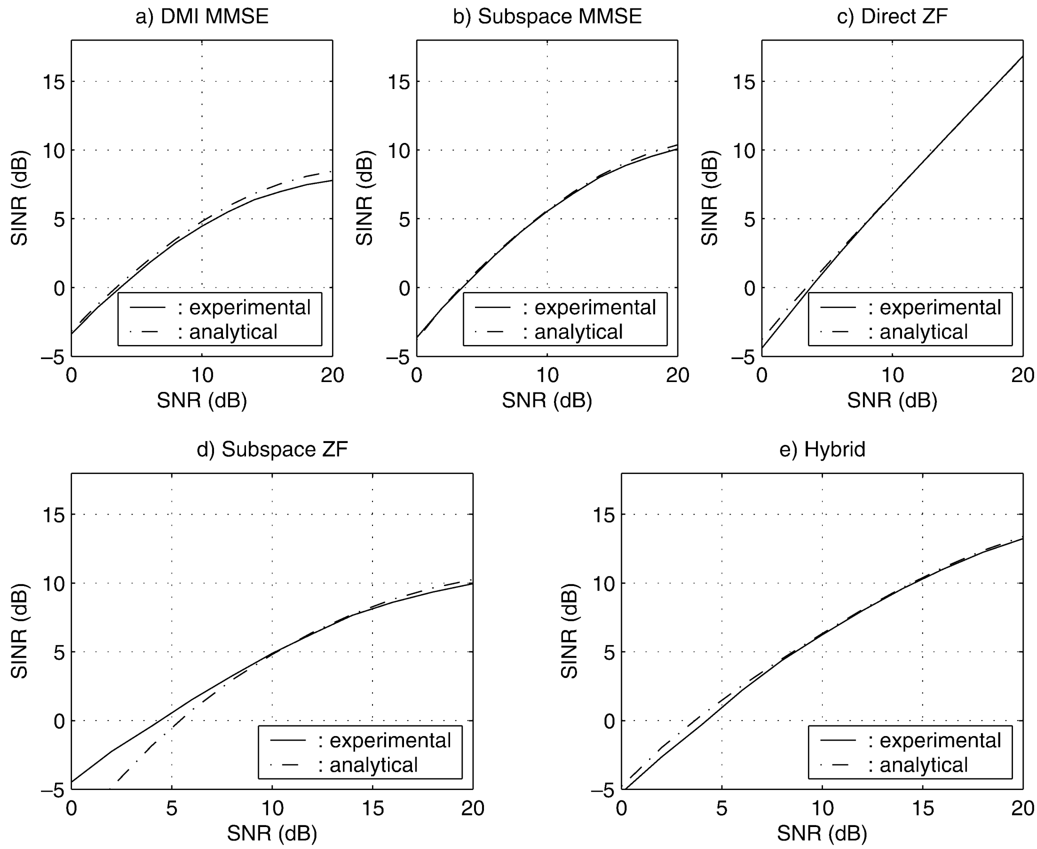

Fig. 6. The average output SINR versus SNR for the DMI MMSE, subspace MMSE, direct ZF, subspace ZF, and hybrid detectors in multipath channels. Channel parameters are estimated by the subspace method. $M = 31, q = 3, J = 15, K = 10, N = 200$.

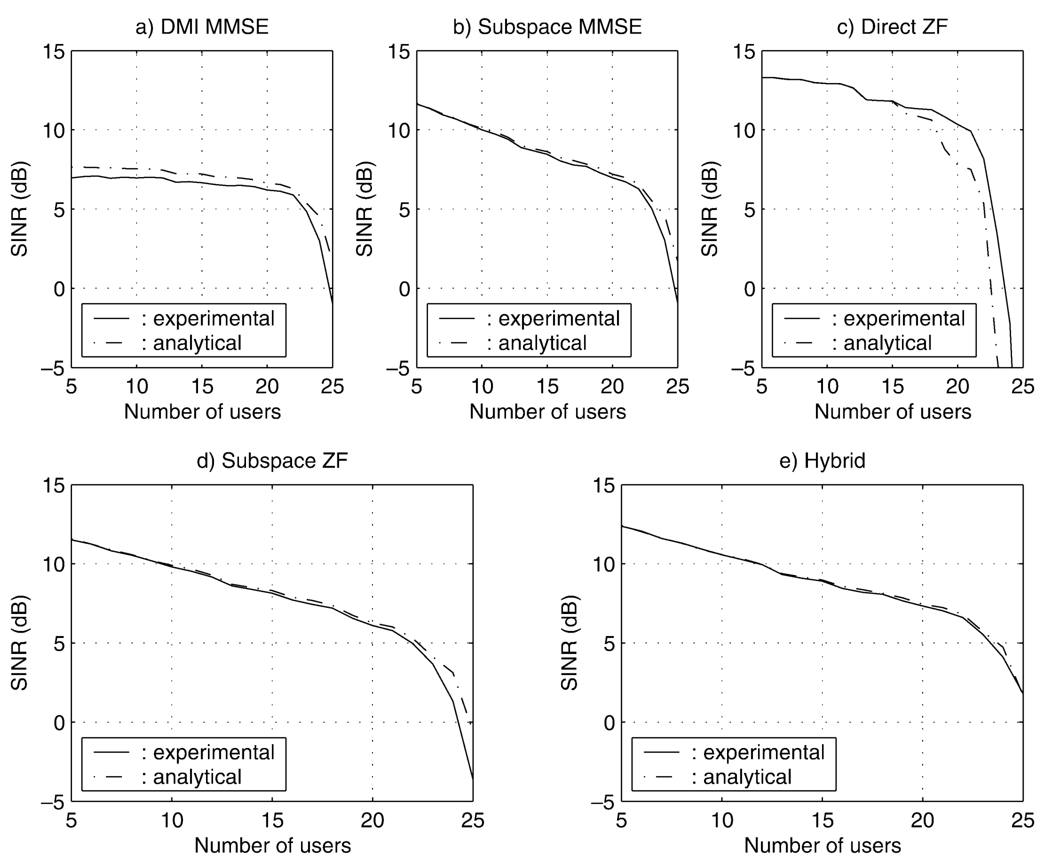

Fig. 7. The average output SINR versus the number of users for the DMI MMSE, subspace MMSE, direct ZF, subspace ZF, and hybrid detectors in multipath channels. Channel parameters are estimated by the subspace method. $M = 31, q = 3, K = 3$, SNR= 15 dB, $N = 200$.

subspace MMSE detectors show similar but a little worse performance. Their performance is better than the DMI MMSE detector.

V. Concluding Remarks

Various blind and group-blind multiuser detectors are analyzed from a perturbation perspective. The results for flat channels are consistent with those from an existing ALT approach. Performance in the presence of multipath distortion is also studied jointly with the subspace channel estimation method. All analyses are tested in different environments and verified by computer simulation.

Appendix
Proof of Proposition

Define $\widehat{\boldsymbol{r}}_n = \mathrm{vec}\left(\boldsymbol{y}_n\boldsymbol{y}_n^H\right)$ as the instantaneous vectorized covariance. Then it can be easily verified that the covariance of $\delta\boldsymbol{r}$ has a form

$$\begin{aligned}\boldsymbol{\Phi}_r &= E\{(\widehat{\boldsymbol{r}}-\boldsymbol{r})(\widehat{\boldsymbol{r}}-\boldsymbol{r})^H\}\\ &= \frac{1}{N^2}\sum_{n_1,n_2=1}^{N} E\left\{\widehat{\boldsymbol{r}}_{n_1}\widehat{\boldsymbol{r}}_{n_2}^H\right\} - \boldsymbol{r}\boldsymbol{r}^H \end{aligned}\tag{56}$$

where we have used $E\{\widehat{\boldsymbol{r}}_{n_1}\} = E\{\widehat{\boldsymbol{r}}_{n_2}\} = \boldsymbol{r}$. Considering all possible values which n_1 and n_2 take, the summation can be expanded into $n_1 = n_2$ and $n_1 \neq n_2$. The latter gives $\frac{1}{N^2}(N^2-N)\boldsymbol{r}\boldsymbol{r}^H$ due to our independence assumption of data vectors used for covariance estimation. Together with the result from the first, (56) becomes

$$N\boldsymbol{\Phi}_r = E\left\{\widehat{\boldsymbol{r}}_n\widehat{\boldsymbol{r}}_n^H\right\} - \boldsymbol{r}\boldsymbol{r}^H. \tag{57}$$

Expressing $\widehat{\boldsymbol{r}}_n$ as $\boldsymbol{y}_n^*\otimes\boldsymbol{y}_n$, (57) becomes

$$N\boldsymbol{\Phi}_r = E\left\{\left(\boldsymbol{y}_n^*\otimes\boldsymbol{y}_n\right)\left(\boldsymbol{y}_n^*\otimes\boldsymbol{y}_n\right)^H\right\} - \boldsymbol{r}\boldsymbol{r}^H. \tag{58}$$

It is necessary to simplify a key term

$$E\left\{\left(\boldsymbol{y}_n^*\otimes\boldsymbol{y}_n\right)\left(\boldsymbol{y}_n^*\otimes\boldsymbol{y}_n\right)^H\right\}$$

in (58). Some results have been derived for complex variables $\boldsymbol{y}_n$ in [23]. We will complete derivation for real variables and reiterate results for complex variables as well for integrity.

Denote elements of $\boldsymbol{y}_n$ by y_i for $i = 1,\dots,\nu$. For a zero-mean vector $\boldsymbol{y}_n$, define the fourth-order cumulant matrix as [23]

$$\boldsymbol{K}_{\boldsymbol{y}} = \sum_{a,b,c,d=1}^{\nu}(\boldsymbol{e}_{\nu,b}\otimes\boldsymbol{e}_{\nu,a})(\boldsymbol{e}_{\nu,c}\otimes\boldsymbol{e}_{\nu,d})^T\mathrm{cum}\,(y_a,y_b^*,y_c,y_d^*)$$

where

$$\begin{aligned}\mathrm{cum}\,(y_a,y_b^*,y_c,y_d^*) = E\,&\{y_ay_b^*y_cy_d^*\}\\ &- E\,\{y_ay_b^*\}E\{y_cy_d^*\}\\ &- E\,\{y_ay_d^*\}\,E\,\{y_b^*y_c\}\\ &- E\{y_ay_c\}E\,\{y_b^*y_d^*\}\,.\end{aligned}$$

It can be written compactly as [23]

$$\begin{aligned}\boldsymbol{K}_{\boldsymbol{y}} = &E\left\{\left(\boldsymbol{y}_n^*\otimes\boldsymbol{y}_n\right)\left(\boldsymbol{y}_n^T\otimes\boldsymbol{y}_n^H\right)\right\}\\ &- E\left\{\boldsymbol{y}_n^*\otimes\boldsymbol{y}_n\right\}E\left\{\boldsymbol{y}_n^T\otimes\boldsymbol{y}_n^H\right\}\\ &- E\left\{\boldsymbol{y}_n^*\boldsymbol{y}_n^T\right\}\otimes E\left\{\boldsymbol{y}_n\boldsymbol{y}_n^H\right\}\\ &- E\left\{(\boldsymbol{y}_n^*\otimes\boldsymbol{1}_\nu)(\boldsymbol{1}_\nu\otimes\boldsymbol{y}_n)^H\right\}\\ &\odot E\left\{(\boldsymbol{1}_\nu\otimes\boldsymbol{y}_n)(\boldsymbol{y}_n^*\otimes\boldsymbol{1}_\nu)^H\right\}\end{aligned}\tag{59}$$

from which we obtain

$$\begin{aligned}E\left\{\left(\boldsymbol{y}_n^*\otimes\boldsymbol{y}_n\right)\left(\boldsymbol{y}_n^T\otimes\boldsymbol{y}_n^H\right)\right\} = &\boldsymbol{K}_{\boldsymbol{y}}\\ &+ E\left\{\boldsymbol{y}_n^*\otimes\boldsymbol{y}_n\right\}E\left\{\boldsymbol{y}_n^T\otimes\boldsymbol{y}_n^H\right\}\\ &+ E\left\{\boldsymbol{y}_n^*\boldsymbol{y}_n^T\right\}\otimes E\left\{\boldsymbol{y}_n\boldsymbol{y}_n^H\right\}\\ &+ E\left\{\left(\boldsymbol{y}_n^*\otimes\boldsymbol{1}_\nu\right)\left(\boldsymbol{1}_\nu\otimes\boldsymbol{y}_n\right)^H\right\}\\ &\odot E\left\{\left(\boldsymbol{1}_\nu\otimes\boldsymbol{y}_n\right)\left(\boldsymbol{y}_n^*\otimes\boldsymbol{1}_\nu\right)^H\right\}.\end{aligned}\tag{60}$$

We will simplify (60) term by term next.

According to data model (6), the first term becomes [22]

$$\boldsymbol{K}_{\boldsymbol{y}} = (\boldsymbol{H}^*\otimes\boldsymbol{H})\boldsymbol{K}_{\boldsymbol{b}}(\boldsymbol{H}^*\otimes\boldsymbol{H})^H + \boldsymbol{K}_{\boldsymbol{v}}. \tag{61}$$

For Gaussian noise, $\boldsymbol{K}_{\boldsymbol{v}} = \boldsymbol{0}$, while for μ independent inputs

$$\begin{aligned}\boldsymbol{K}_{\boldsymbol{b}} &= \sum_{i=1}^{\mu}\kappa_i(\boldsymbol{e}_{\mu,i}\otimes\boldsymbol{e}_{\mu,i})(\boldsymbol{e}_{\mu,i}\otimes\boldsymbol{e}_{\mu,i})^T\\ &= (\boldsymbol{I}_\mu\Box\boldsymbol{I}_\mu)\mathrm{diag}\{\kappa_1,\dots,\kappa_\mu\}(\boldsymbol{I}_\mu\Box\boldsymbol{I}_\mu)^T\end{aligned}\tag{62}$$

where $\boldsymbol{e}_{\mu,i}$ is the ith column of identity matrix $\boldsymbol{I}_\mu$, κ_i is the kurtosis (fourth-order autocumulant) of the ith input. If all inputs have the same kurtosis κ_{4b}, after substituting (62) into (61) and applying the following property [21]:

$$(\boldsymbol{A}_1\otimes\boldsymbol{A}_2)(\boldsymbol{A}_3\Box\boldsymbol{A}_4) = (\boldsymbol{A}_1\boldsymbol{A}_3)\Box(\boldsymbol{A}_2\boldsymbol{A}_4)$$

we obtain

$$\boldsymbol{K}_{\boldsymbol{y}} = \kappa_{4b}(\boldsymbol{H}^*\Box\boldsymbol{H})(\boldsymbol{H}^*\Box\boldsymbol{H})^H. \tag{63}$$

The second term of (60) can be easily observed to be $\boldsymbol{r}\boldsymbol{r}^H$. The third term is simplified as $\boldsymbol{R}^*\otimes\boldsymbol{R}$. The last term vanishes for complex variables [23]. For real variables, its first half becomes

$$\begin{aligned}E\left\{\left(\boldsymbol{y}_n\otimes\boldsymbol{1}_\nu\right)\left(\boldsymbol{1}_\nu^T\otimes\boldsymbol{y}_n^T\right)\right\} &= E\left\{\left(\boldsymbol{I}_\nu\boldsymbol{y}_n\otimes\boldsymbol{1}_\nu\right)\left(\boldsymbol{1}_\nu^T\otimes\boldsymbol{y}_n^T\boldsymbol{I}_\nu\right)\right\}\\ &= E\Big\{(\boldsymbol{I}_\nu\otimes\boldsymbol{1}_\nu)(\boldsymbol{y}_n\otimes 1)\\ &\qquad\times\left(1\otimes\boldsymbol{y}_n^T\right)\left(\boldsymbol{1}_\nu^T\otimes\boldsymbol{I}_\nu\right)\Big\}\\ &= (\boldsymbol{I}_\nu\otimes\boldsymbol{1}_\nu)E\left\{\boldsymbol{y}_n\boldsymbol{y}_n^T\right\}\left(\boldsymbol{1}_\nu^T\otimes\boldsymbol{I}_\nu\right)\\ &= (\boldsymbol{I}_\nu\otimes\boldsymbol{1}_\nu)\boldsymbol{R}\left(\boldsymbol{1}_\nu^T\otimes\boldsymbol{I}_\nu\right)\end{aligned}\tag{64}$$

where both vector $\mathbf{1}_\nu$ and scalar 1 are involved in the second equality. Similarly, the second half of the last term of (60) can be simplified as

$$E\left\{(\mathbf{1}_\nu \otimes \boldsymbol{y}_n)\left(\boldsymbol{y}_n^T \otimes \mathbf{1}_\nu^T\right)\right\} = (\mathbf{1}_\nu \otimes \boldsymbol{I}_\nu)\boldsymbol{R}\left(\boldsymbol{I}_\nu \otimes \mathbf{1}_\nu^T\right). \quad (65)$$

Combining all previously derived results, we have for real variables

$$\begin{aligned} E\left\{(\boldsymbol{y}_n^* \otimes \boldsymbol{y}_n)\left(\boldsymbol{y}_n^T \otimes \boldsymbol{y}_n^H\right)\right\} = &\, \kappa_{4b}(\boldsymbol{H}\Box\boldsymbol{H})(\boldsymbol{H}\Box\boldsymbol{H})^T \\ &+ \boldsymbol{r}\boldsymbol{r}^T + \boldsymbol{R}\otimes\boldsymbol{R} \\ &+ \left[(\boldsymbol{I}_\nu \otimes \mathbf{1}_\nu)\boldsymbol{R}\left(\mathbf{1}_\nu^T \otimes \boldsymbol{I}_\nu\right)\right] \\ &\odot (\mathbf{1}_\nu \otimes \boldsymbol{I}_\nu)\boldsymbol{R}\left(\boldsymbol{I}_\nu \otimes \mathbf{1}_\nu^T\right), \end{aligned} \quad (66)$$

while for complex variables

$$\begin{aligned} E\left\{(\boldsymbol{y}_n^* \otimes \boldsymbol{y}_n)\left(\boldsymbol{y}_n^T \otimes \boldsymbol{y}_n^H\right)\right\} = &\, \kappa_{4b}(\boldsymbol{H}^*\Box\boldsymbol{H})(\boldsymbol{H}^*\Box\boldsymbol{H})^H \\ &+ \boldsymbol{r}\boldsymbol{r}^H + \boldsymbol{R}^*\otimes\boldsymbol{R}. \end{aligned} \quad (67)$$

Therefore, (36) and (37) follow immediately after (58), (66), and (67) are considered.

REFERENCES

[1] M. Honig, U. Madhow, and S. Verdú, "Blind adaptive multiuser detection," *IEEE Trans. Inform. Theory*, vol. 41, pp. 944–960, July 1995.

[2] X. Wang and H. V. Poor, "Blind multiuser detection: A subspace approach," *IEEE Trans. Inform. Theory*, vol. 44, pp. 677–690, Mar. 1998.

[3] M. Tsatsanis and Z. Xu, "Performance analysis of minimum variance CDMA receivers," *IEEE Trans. Signal Processing*, vol. 46, pp. 3014–3022, Nov. 1998.

[4] Z. Xu and M. Tsatsanis, "Blind adaptive algorithms for minimum variance CDMA receivers," *IEEE Trans. Commun.*, vol. 49, pp. 180–194, Jan. 2001.

[5] M. Honig, S. Miller, M. Shensa, and L. Milstein, "Performance of adaptive linear interference suppression in the presence of dynamic fading," *IEEE Trans. Commun.*, vol. 49, pp. 635–45, Apr. 2001.

[6] S. Verdú, *Multiuser Detection*. Cambridge, U.K.: Cambridge Univ. Press, 1998.

[7] X. Wang and H. V. Poor, "Blind equalization and multiuser detection in dispersive CDMA channels," *IEEE Trans. Commun.*, vol. 46, pp. 91–103, Jan. 1998.

[8] X. Wang and A. Høst-Madsen, "Group-blind multiuser detection in uplink CDMA," *IEEE J. Select. Areas Commun.*, vol. 17, pp. 1971–1984, Nov. 1999.

[9] M. Torlak and G. Xu, "Blind multiuser channel estimation in asynchronous CDMA systems," *IEEE Trans. Signal Processing*, vol. 45, pp. 137–147, Jan. 1997.

[10] J. Chen and U. Mitra, "Optimum near-far resistance for dual-rate DS/CDMA signals: Random signature sequence analysis," *IEEE Trans. Inform. Theory*, vol. 45, pp. 2434–2447, Nov. 1999.

[11] M. Honig and W. Xiao, "Large system performance of reduced-rank linear filters," in *Proc. 37th Annu. Allerton Conf. Communications, Computing and Control*, Monticello, IL, Sept. 1999.

[12] U. Madhow and M. Honig, "On the average near–far resistance for MMSE detection of direct sequence CDMA signals with random spreading," *IEEE Trans. Inform. Theory*, vol. 45, pp. 2039–2045, Nov. 1999.

[13] S. Verdú and S. Shamai (Shitz), "Spectral efficiency of CDMA with random spreading," *IEEE Trans. Inform. Theory*, vol. 45, pp. 622–640, Mar. 1999.

[14] J. Zhang and X. Wang, "Large-system performance analysis of blind and group-blind multiuser receivers," *IEEE Trans. Inform. Theory*, vol. 48, pp. 2507–2523, Sept. 2002.

[15] A. Høst-Madsen and X. Wang, "Performance of blind and group-blind multiuser detectors," *IEEE Trans. Inform. Theory*, vol. 48, pp. 1849–1872, July 2002.

[16] F. Li, H. Liu, and R. Vaccaro, "Performance analysis for DOA estimation algorithms: Unification, simplification, and observations," *IEEE Trans. Aerosp. Electron. Syst.*, vol. 29, no. 4, pp. 1170–1184, Oct. 1993.

[17] Z. Xu, "Asymptotic performance of subspace methods for synchronous multirate CDMA systems," *IEEE Trans. Signal Processing*, vol. 50, pp. 2015–2026, Aug. 2002.

[18] ——, "Perturbation analysis for subspace decomposition with applications in subspace-based algorithms," *IEEE Trans. Signal Processing*, vol. 50, pp. 2820–2830, Nov. 2002.

[19] ——, "On the second-order statistics of the weighted sample covariance matrix," *IEEE Trans. Signal Processing*, vol. 51, pp. 527–534, Feb. 2003.

[20] S. Bensley and B. Aazhang, "Subspace-based channel estimation for code division multiple access communication systems," *IEEE Trans. Commun.*, vol. 44, pp. 1009–1020, Aug. 1996.

[21] H. Van Trees, *Optimum Array Processing: Part IV of Detection, Estimation and Modulation Theory*. New York: Wiley, 2002.

[22] G. B. Giannakis, Y. Hua, P. Stoica, and L. Tong, *Signal Processing Advances in Wireless & Mobile Communications: Trends in Single- and Multi-User Systems*. Saddle Brook, NJ: Prentice Hall, 2001, ch. 3.

[23] A. J. van der Veen, "Statistical performance analaysis of the algebraic constant modulus algorithm," *IEEE Trans. Signal Processing*, vol. 50, pp. 3083–3097, Dec. 2002.